

**Toward a metabolic understanding of 2-aminoacrylate stress in *ridA* mutants of
*Salmonella enterica***

By

Jeffrey M. Flynn

A dissertation submitted in partial fulfillment of
the requirements for the degree of

Doctor of Philosophy
(Microbiology)

at the

UNIVERSITY OF WISCONSIN-MADISON

2013

Date of final oral examination: 5/16/13

This dissertation is approved by the following members of the Final Oral Committee:
Diana M. Downs, Professor, Bacteriology
Michael G. Thomas, Associate Professor, Bacteriology
Brian G. Fox, Professor, Biochemistry
Heidi Goodrich-Blair, Professor, Bacteriology
Paul J. Weimer, Associate Professor, Bacteriology

ABSTRACT

Thorough study of cellular metabolism reveals that evolution has favored the advent of useful enzymologies despite deleterious consequences they may pose. Molecular oxygen biochemistry exemplifies this paradigm and proves indispensable and unavoidable for much of life despite the toxic products intrinsic to its utilization. Enzymes evolved to neutralize the reactive oxygen species inherent in aerobic environments; superoxide dismutase and catalase are nearly ubiquitous enzymes amongst aerobic organisms. Subsequently, it can be said that the evolution of efficient metabolism requires the balance of useful catalysis with the development of means to neutralize any inherent toxic products and byproducts.

Much effort has been put toward understanding pathways used to utilize substrates for carbon or nitrogen and pathways used to synthesize compounds needed for cellular life. These efforts have generated an exquisite map of canonical metabolic reactions. However subtle, low-flux connections between these pathways have gone unnoticed. In the same way, toxic metabolites inherent to certain reactions may have never been uncovered in the laboratory due to their subtle effects. These subtle effects, however, have a profound impact in the evolutionary pressures of the real world.

The story presented here is one such paradigm of a toxic metabolite, 2-aminoacrylate (2-AA), and the enzyme responsible for its neutralization, RidA. The endogenous production of 2-AA and the role of RidA to neutralize it have been overlooked and misunderstood until recently. The current model is that 2-AA is generated by some metabolic enzymes and can, in the absence of RidA, accumulate and inactivate a different set of metabolic enzymes.

The story of RidA is complicated and nuanced, drawing together far-reaching areas of the

metabolic network, and has uncovered more details about the complex cellular milieu. This work used *Salmonella enterica* to show the intimate connection of the highly conserved RidA family to pyridoxal 5'-phosphate (PLP) enzymology. RidA protects the PLP-containing enzymes alanine racemase and serine hydroxymethyltransferase from damage via 2-AA generated from the PLP-enzyme threonine dehydratase, preserving alanine and one-carbon metabolisms.

ACKNOWLEDGEMENTS

No scientific work is done from a clean slate or in a vacuum. I thank all who have toiled before me in the scientific community whose work I use as a basis for my own efforts. For those who work around and with me – your work, thoughtful discussion, and mutual interest continue to motivate me in this pursuit; thank you. All the Downs lab members past and present have enriched my life scientifically and personally, you have become like family to me and I thank you for welcoming me and providing an amazing environment to come to everyday.

Thank you to my mentor, Diana, who has both put up with my idiosyncrasies and had confidence in my abilities when my poise waned. Thank you for working tirelessly to ensure that my best interests were sought and motivating me when times were bleak. Your energy, effort and enthusiasm are a model for me in life and my career.

Thank you to Michael Thomas for acting as a surrogate mentor, taking me into your lab without hesitation and entertaining all my conversations, scientific or otherwise. Your efforts and successes in scientific education are an inspiration.

My friends and family have been amazing throughout this whole process. Thank you for your encouragement and your excitement. The most thanks goes to my wife, Chelsea, without her I would not have completed this degree. Chelsea, I cannot begin to repay your support throughout this process; you were overly patient, kind and supportive as science controlled and consumed much of my life over these years.

I hope that my young son, Isaac, finds this manuscript one day and it sparks his curiosity. My strongest desire for you is that you pursue all of your endeavors with a tireless enthusiasm.

TABLE OF CONTENTS

Abstract	i
Acknowledgements	iii
List of Tables	ix
List of Figures	x
CHAPTER 1: Introduction	1
1.1 RidA background	1
1.2 RidA activity and enamine chemistry	2
1.3 2-aminoacrylate chemistry, production, and inhibition of PLP- enzymes	6
1.4 Overall model of 2-AA damage in <i>ridA</i> mutants	8
1.5 PLP enzymes	10
1.6 One carbon metabolism	10
1.7 Dissertation outline	12
1.8 References	13
CHAPTER 2: In the Absence of RidA, Endogenous 2-Aminoacrylate Inactivates Alanine Racemase by Modifying the Pyridoxal 5'-Phosphate Cofactor	18
2.1 Abstract	19
2.2 Introduction	19
2.3 Materials and methods	23
2.3.1 Bacterial strains, media, and chemicals	23

2.3.2 Molecular biology – Construction of pJF2	24
2.3.3 Alanine racemase assay – Crude extract	25
2.3.4 Alanine racemase assay – Purified protein	26
2.3.5 Protein purification	26
2.3.6 Characterization of cofactor content	27
2.3.7 Mass spectroscopy of cofactor	28
2.4 Results and Discussion	28
2.4.1 <i>ridA</i> mutants are compromised in L-alanine utilization	29
2.4.2 Alanine racemase activity is compromised in <i>ridA</i> mutant. strains	31
2.4.3 Isoleucine addition corrects growth defect of RidA deficient strains	32
2.4.4 Alr protein purified from <i>ridA</i> cells is modified	33
2.5 Conclusions	36
2.7 References	38
CHAPTER 3: Decreased coenzyme A levels in <i>ridA</i> mutant strains of <i>Salmonella</i> <i>enterica</i> result from inactivated serine hydroxymethyltransferase	43
3.1 Abstract	44
3.2 Introduction	44
3.3 Materials and methods	46
3.3.1 Bacterial strains, media, and chemicals	46
3.3.2 Molecular biology – Construction of JF4	47
3.3.3 Ketoacid detection	47

3.3.4 HPLC separation of ketoacids and mass spectral analysis	48
3.3.5 Detection of pyruvate in culture supernatants	49
3.3.6 Determination of total coenzyme A in cells	49
3.3.7 Serine hydroxymethyltransferase activity	50
3.3.8 Serine hydroxymethyltransferase purification	51
3.4 Results and discussion	51
3.4.1 Ketoacids accumulate in growth media of <i>ridA</i> mutant strains	51
3.4.2 Mutants lacking RidA accumulate pyruvate due to lowered coenzyme A levels	53
3.4.3 Lowered CoA levels in <i>ridA</i> mutants are due to a defect in one-carbon metabolism	58
3.4.4 <i>ridA</i> mutants have lowered serine hydroxymethyltransferase activity	59
3.4.5 GlyA isolated from a <i>ridA</i> strain had reduced specific activity and distinct spectral characteristics	59
3.4.6 Threonine dehydratase activity is responsible for decreasing GlyA activity	63
3.5 Conclusions	64
3.6 References	65
CHAPTER 4: Summary, Conclusions, Future Directions, and Final Comments.	70
4.1. Summary and conclusions	70

4.1.1 Overview	70
4.1.2 <i>ridA</i> mutants contain 2-aminoacrylate-modified Alr enzymes	70
4.1.3 <i>ridA</i> mutants excrete pyruvate due to a compromised serine hydroxymethyltransferase activity	71
4.2 Future directions	72
4.2.1 Serine metabolism and leucine responsive protein	72
4.2.2 Identification of new targets of 2-aminoacrylate inhibition	75
4.3 Final comments	76
4.4 References	78
APPENDIX A: Structural explorations in RidA mechanism	80
A1. Introduction	81
A2. TdcF crystal structure	82
A3. RidA activity in light of TdcF crystal structure	83
A4. Future directions	86
A5. References	87
APPENDIX B: The construction of a strain that accumulates 2-aminoacrylate gives evidence for phosphohydroxythreonine transaminase inhibition	89
B.1. Introduction	90
B.2. Materials and methods	91
B.2.1. Bacterial strains, media and chemicals	91
B.2.2. Molecular biology	91
B.2.3. HPLC quantification of cofactors	92

B.3. Results	92
B.3.1. Construction of strain for the inducible expression of <i>tdcB</i>	92
B.3.2. Strains expressing <i>tdcB</i> result in greater 2-AA accumulation in <i>ridA</i> mutant strains	94
B.4. Conclusions and future directions	95
B.5. References	96

LIST OF TABLES**Chapter 2**

Table 2.1. Bacterial strains 24

Table 2.2. Alanine racemase activity in permeablized cells 32

Chapter 3

Table 3.1. Bacterial strains 47

Table 3.2. Total CoA levels are lowered in *ridA* strain 57

Table 3.3. Serine hydroxymethyltransferase activity in crude extract 59

Appendix B

Table B.1. Cofactor content of Alr isolated from various strains 95

LIST OF FIGURES

Chapter 1

- Figure 1.1. Mechanism of 2-aminocrotonate tautamerization and hydrolysis/
deamination to 2-ketobutyrate 3
- Figure 1.2. Energy state diagram of the breakdown of aminocrotonate in aqueous
solution 4
- Figure 1.3. The pH profile of IlvA-mediated production of 2-ketobutyrate from
L-threonine shifts in the presence of RidA 5
- Figure 1.4. Mechanism of 2-aminoacrylate-mediated inactivation 7
- Figure 1.5. Model for *in vivo* role of RidA 9
- Figure 1.6. One-carbon unit generation 11

Chapter 2

- Figure 2.1. Catalytic mechanism of alanine racemase and mechanism of 2-aminoacrylate
inhibition in Alr 21-22
- Figure 2.2. *ridA* mutants are compromised in the utilization of L-alanine as a nitrogen
source 30
- Figure 2.3. Alr isolated from *ridA* strain contains multiple cofactors 34
- Figure 2.4. Alr isolated from *ridA* strain contains 2-aminoacrylate modified cofactor 35

Chapter 3

- Figure 3.1. Ketoacids accumulate in the culture medium of *ridA* mutant strains 52
- Figure 3.2. The metabolic interconnection of glycolysis, one-carbon metabolism, valine
biosynthesis and pantothenate biosynthesis 54

Figure 3.3. <i>ridA</i> mutants excrete pyruvate	56
Figure 3.4. Spectral characteristics of <i>ridA</i> -isolated GlyA differ from wild type-isolated GlyA	61
Figure 3.5. GlyA active site configuration and proposed modification scheme	62
Chapter 4	
Figure 4.1. Serine metabolic node	74
Appendix A	
Figure A.1. The active site configuration of TdcF	82
Figure A.2. Proposed mechanism of RidA catalysis of 2-aminocrotonate to 2-ketobutyrate	84
Figure A.3. Activity of RidA variants.	85
Figure A.4. The proposed structural analog of the reaction intermediate	87
Appendix B	
Figure B.1. pJF5 map	93

CHAPTER 1

INTRODUCTION

1.1. RidA Background

The Downs lab has used classical genetics and biochemical approaches to uncover connections between disparate areas of metabolism. Much effort has used thiamine biosynthesis in *Salmonella enterica* as a tool to probe connections between metabolic pathways. The low demand for thiamine in the cell makes it a sensitive indicator for flux across the metabolic network or “crosstalk” whereby non-canonical pathways can form to generate substrates required for growth.

To elucidate instances of crosstalk, suppressor mutants were isolated that grow in the absence of the thiamine and purine biosynthetic enzyme amidophosphoribosyltransferase, PurF. The most common suppressor mutation that was isolated was a *ridA* null mutant [1]. *In vitro* and *in vivo* characterizations demonstrated that in the absence of PurF and RidA the tryptophan biosynthetic enzyme, anthranilate phosphoribosyltransferase (TrpD), is able to use the reactive enamine 2-aminocrotonate as a nitrogen donor for the synthesis of the thiamine precursor phosphoribosylamine (PRA) [2, 3]. In contrast, the presence of RidA activity prevented the formation of PRA *in vitro* by expediting the breakdown of 2-aminocrotonate [2]. It follows that if RidA is present in the cell, 2-aminocrotonate does not accumulate and cannot be used for PRA synthesis. This story provides a representative example of metabolic crosstalk: an unknown cellular flux was revealed by the cell compensating for the lack of a thiamine biosynthetic enzyme (PurF) by using an isoleucine precursor (2-aminocrotonate generated from threonine) and an activity from a tryptophan synthesis enzyme (TrpD) to generate a required metabolite for growth.

The loss of RidA did not only allow for the production of thiamine in a *purF* mutant but also causes pleiotropic phenotypes [4]. These phenotypes include conditional sensitivities to serine and cysteine, a deficiency in isoleucine biosynthesis [5], and slow growth utilizing pyruvate as a carbon source [6]. The diversity of the phenotypes and the subtle nature of their presentation have made the elucidation of RidA function difficult.

A survey of sequenced genomes reveals that the RidA (YjgF/YER057c/UK114) family has representatives in all domains of life [7, 8] and can be found operons encoding enzymes for biosynthetic pathways [9] and degradative pathways alike [10]. RidA has been implicated in the diverse cellular processes of isoleucine metabolism [5] and transcription initiation [11] and has been identified as a tumor antigen [12]. The prevalence of this protein family suggested an important physiological role and subsequently much effort (structural studies, metabolic probing, and molecule screening) has focused on elucidating a role for the family *in vivo*.

1.2. RidA Activity and Enamine Chemistry

Recent work in our laboratory revealed an activity for the RidA enzyme family, connecting it to certain types of pyridoxal 5'-phosphate (PLP)-enzyme products [13]. RidA increases the rate of hydrolysis of the unstable enamines 2-AA and 2-aminocrotonate, products generated within the cell by PLP-dependent dehydratases [14, 15] and amino acid oxidases [16]. These unstable products are readily hydrolyzed in aqueous solutions, but RidA accelerates this hydrolysis resulting in a significant reduction in the half-life of these enamines *in vitro* [13].

To understand the activity of RidA and the effect of RidA substrates on cellular physiology, a discussion of aminocrotonate chemistry in the absence of RidA will be helpful. Aminocrotonate is an unstable enamine intermediate generated from threonine by threonine

dehydratase, IlvA [17]. The breakdown of aminocrotonate involves two steps: the tautomerization to the imine form, iminobutyrate and the attack by water to hydrolyze and deaminate (Figure 1.1). For the enamine to tautomerize, two steps must happen in a sequential or concerted mechanism: (1) a proton must be abstracted from the amino group freeing the electrons to form the imine bond (Figure 1.1, I) and (2) a pair of electrons from the alpha-beta carbon double bond must pick up a proton (Figure 1.1, II).

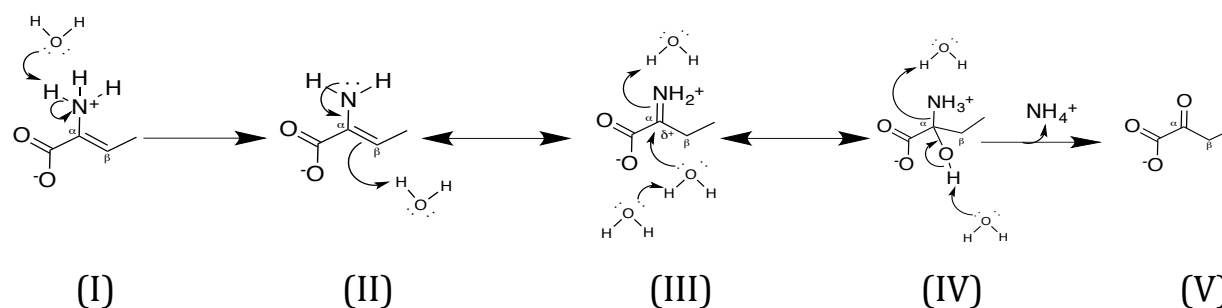


Figure 1.1. Mechanism of 2-aminocrotonate tautomerization and hydrolysis/deamination to 2-ketobutyrate. The mechanism depicted is in water at neutral pH whereby all acids and bases are H_2O . The first step (I) is deprotonating the amino group yielding a lone pair on the nitrogen, subsequently or concertedly with (I) movement of the electrons from the nitrogen to form the imine bond while the beta carbon is protonated (II). The tautomerization makes the alpha carbon more electrophilic and susceptible to attack by water (III) and the intermediate (IV) quickly deaminates to 2-ketobutyrate (V).

The enamine and imine vary in their relative stability and their susceptibility to nucleophilic attack presumably because of the magnitude of the dipole moment at the alpha carbon. In the transition from the enamine to the imine form, the alpha carbon gains a nitrogen bond while losing a carbon bond. Nitrogen has a higher electronegativity so the imine bond has a stronger dipole than the single nitrogen-carbon bond. This greater dipole means two things: (1)

there is an increase in free energy during the transition from enamine to imine (the enamine is more stable) and (2) the alpha carbon is more electrophilic in the imine form and is susceptible to attack by weak electrophiles (i.e. water).

The stability logic is summed in the hypothetical free energy diagram (Figure 1.2) showing relative free energy values where the deprotonation of the amino group from I-II ($\sim pK_a=10.4$) and the tautomerization from II-III require inputs of energy. The hydrolysis/deamination from III-IV is very favorable and results in net release of free energy.

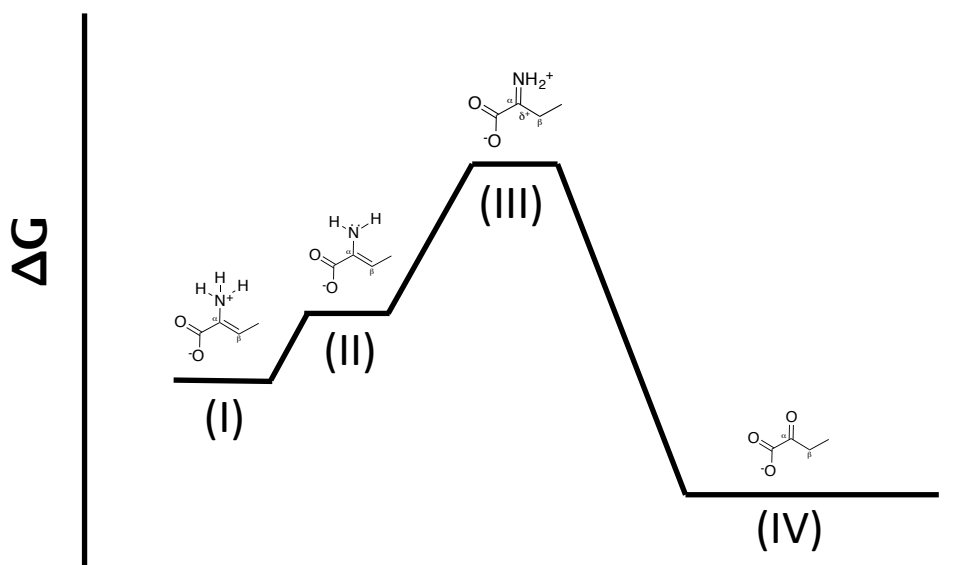


Figure 1.2. Hypothetical energy state diagram of the breakdown of aminocrotonate in aqueous solution. The numbers correspond to reaction mechanism depicted in Figure 1.1 where the deprotonation of the amino group and the tautomerization require energy input and the formation of the final ketoacid is overwhelmingly favorable after the imine is formed in aqueous solutions.

Previous work has shown that increased pH slows the breakdown of the enamine/imine intermediates [17]. The reason for this increase in stability is not immediately apparent, but one can imagine that with decreased availability of protons, the rate limiting tautomerization is hindered because of the weakly acidic character of the beta carbon.

As stated above, RidA accelerates the formation of the ketoacid product from the aminocrotonate intermediate, increasing the already spontaneous hydrolysis in solution alone. This activity was shown using threonine dehydratase, IlvA, to generate aminocrotonate. The figure below (Figure 1.3) is from the seminal RidA activity manuscript [13] and shows that RidA accelerates the formation of 2-ketobutyrate from L-threonine at a range of pH's.

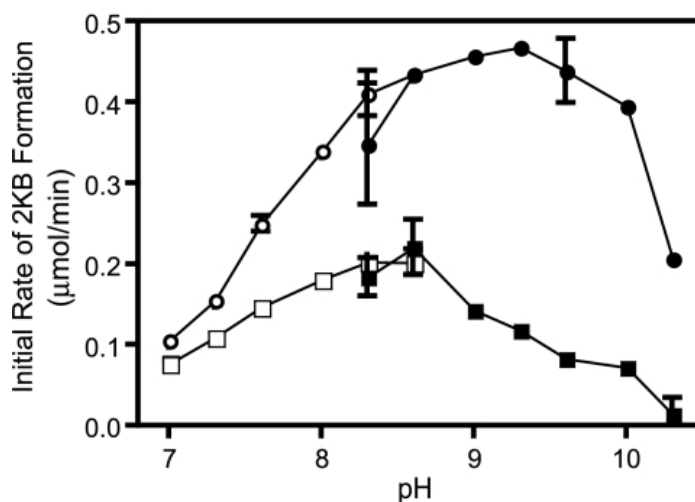


Figure 1.3. The pH profile of IlvA-mediated production of 2-ketobutyrate from L-threonine shifts in the presence of RidA. The initial rate of 2KB formation from 15mM L-threonine with IlvA alone (*squares*) and IlvA + RidA (*circles*) was monitored over a range of pHs. Buffers are 50 mM each MES/HEPES/TAPS (open symbols) and TAPS/CHES/CAPS (closed symbols). *Figure from Lambrect, Flynn and Downs, 2012 [13].*

It can also be seen that the addition of RidA shifts the pH at which maximum rate occurs. In the absence of RidA, the maximum initial rate is at 8.5; however, the addition of RidA results in a shift to pH 9.5. Since the enamine is stabilized at high pH's and the action of RidA is most apparent at high pH's, we hypothesize that RidA facilitates the tautomerization and the hydrolysis, or circumvents the requirement for tautomerization in the hydrolysis. The manner in which RidA facilitates this activity is discussed in Appendix 1 which involves an in depth look at crystal structures of the RidA homolog, TdcF.

1.3. 2-aminoacrylate chemistry, production, and inhibition of PLP-enzymes

The study above detailing RidA activity focused on 2-aminocrotonate deaminase activity but it also demonstrated that RidA has deaminase activity *in vitro* for 2-AA generated from serine. The work presented in this thesis and elsewhere [18] show that one relevant *in vivo* activity of RidA is to deaminate 2-AA. In aqueous solutions, 2-AA is subject to spontaneous hydrolysis, being even more unstable than 2-aminocrotonate; the estimated half-life of 2-AA is ~1.5 seconds at neutral pH [15]. The degradation of 2-AA proceeds similar to 2-aminocrotonate: first 2-AA tautomerizes to its cognate imine, iminopropionate, which is liable to attack and deamination by water.

2-AA has been characterized in a number of biochemical reactions *in vitro*. It is generated and used as an electrophile in the synthesis of cysteine and tryptophan from *o*-acetylserine and serine, respectively [19, 20]. 2-AA is also generated in the PLP-catalyzed degradation of amino acids: tryptophan via tryptophanase, serine via threonine/serine dehydratase, and cysteine via cysteine synthase [17, 21, 22]. 2-AA has additionally been shown to be produced by amino acid oxidases [16]. Subsequently, the production of 2-AA by a number of cellular enzymes has been known, however the implications of 2-AA generation within the

cell have not been investigated.

In addition to being used and generated by certain PLP-enzyme reactions, 2-AA is a well characterized inhibitor of certain PLP-containing enzymes. Small amino acids with good leaving groups on the β -carbon, such as 3-chloroalanine, are enzymatically converted to 2-AA [23-27]. Once generated, the 2-AA covalently modifies a subset of enzymes via the two mechanisms shown in Figure 1.4 [23-31]. The inactivation scheme shown in Figure 1.4.A shows an external aldimine of 2-AA is subject to nucleophilic attack. Nucleophilic side chains in the active site (glutamate, aspartate or cysteine) can attack the external aldimine and result in a covalent modification of the active site residue. The second route depicted in Figure 1.4.B shows 2-AA can attack the PLP internal aldimine in the active site, resulting in a covalent inactivation of the cofactor. Both of these result in a stable covalent modification inhibiting further enzyme function. The multiple routes of inhibition suggest that the active site configuration determines the susceptibility to, and mechanism of, inactivation via 2-AA.

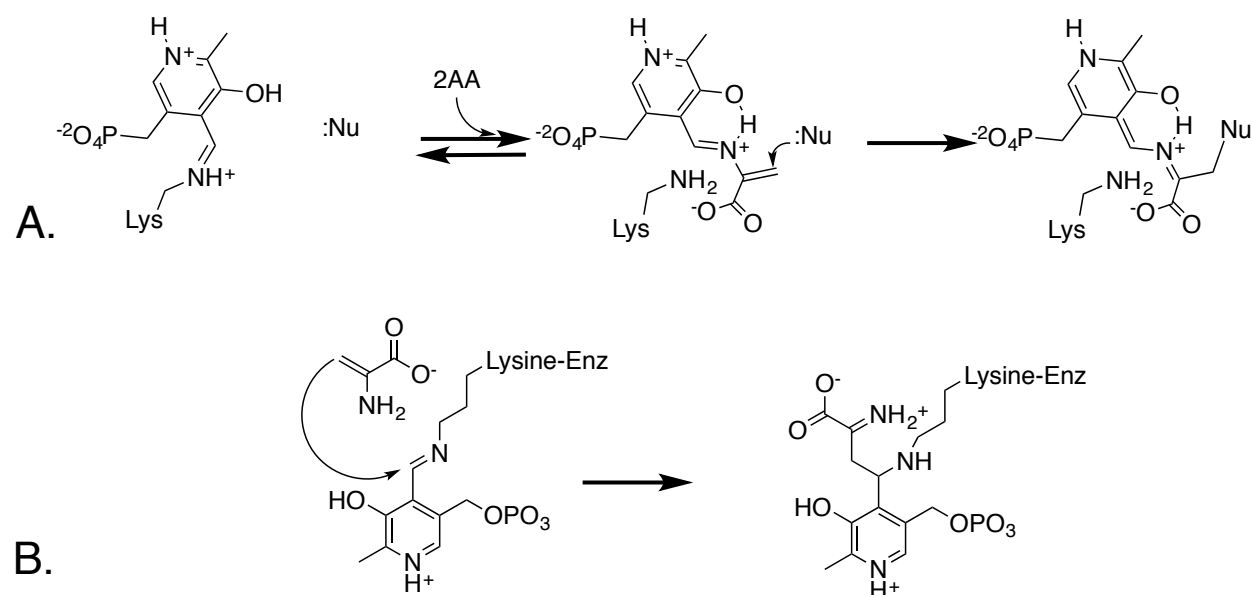


Figure 1.4. Mechanism of 2-aminoacrylate-mediated inactivation. (A) 2-AA first forms an

external aldimine with the PLP, then a nucleophilic attack by an acidic residue near the active site forms a stable adduct. (B) 2-AA attacks the PLP-lysine internal aldimine.

1.4. Overall Model of 2-AA damage in *ridA* mutants

The model for the *in vivo* role for RidA is shown in Figure 1.5. The enamine deaminase activity strongly supported a role of RidA in keeping 2-AA low in the cell and this is corroborated by the studies here and elsewhere [18] demonstrating the accumulation of 2-AA in *ridA* mutant strains. Four enzymes have been shown to be inactivated in the absence of RidA to date: branched chain amino acid transaminase (IlvE) [5, 18], serine hydroxymethyltransferase (GlyA) (*Chapter 3*), degradative alanine racemase (DadX), and the biosynthetic alanine racemase (Alr) (*Chapter 2*). Each of these enzymes is inhibited when the *ridA* mutant strain is grown in minimal medium in the absence of any additional substances. These results demonstrate that 2-AA is produced under normal cellular growth and can accumulate within the cell to levels that are detrimental.

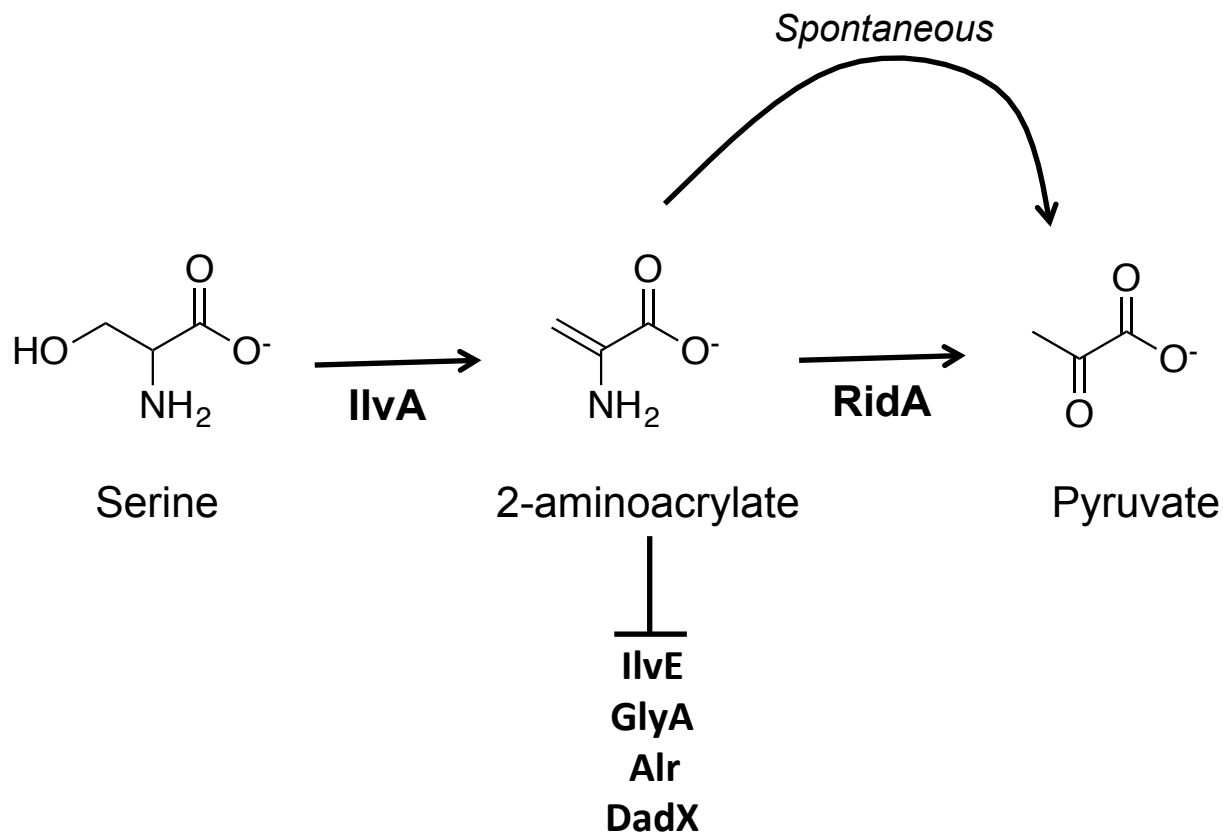


Figure 1.5. Model for *in vivo* role of RidA. 2-AA generated by the biosynthetic threonine dehydratase, IlvA, is broken down both spontaneously and via RidA in the cell. When RidA is absent, 2-AA accumulates and inhibits transaminase C (IlvE), serine hydroxymethyltransferase (GlyA), and the alanine racemases (Alr and DadX).

The population of endogenous 2-AA producers *in vivo* is not yet clear. Supplementation of strains with isoleucine decreases inhibition of the target enzymes. This is consistent with production of 2-AA from serine via the biosynthetic threonine dehydratase, IlvA. IlvA generates 2-AA that can inactivate IlvE *in vitro* and is feedback inhibited by isoleucine [18]. The addition of isoleucine only corrects about ~50% of the defect in the case of IlvE [5] and GlyA, suggesting that enzymes other than IlvA contribute to the production of 2-AA under these conditions.

Further research must be conducted to identify the multitude of enzymes inhibited *in vivo* by 2-AA and the enzymes responsible for its generation.

1.5. PLP Enzymes

Pyridoxal-5'-phosphate (PLP), the coenzyme form of vitamin B₆, is an essential cofactor for the biosynthesis and manipulation of amino acids, amino acid derived metabolites, amino sugars, and amine-containing compounds. PLP enzymes catalyze deamination, decarboxylation, transamination, racemization, and transulfuration reactions [14].

The UV/VIS absorbance spectral properties of PLP-containing enzymes have allowed for ease of *in vitro* study. Therefore, PLP enzyme chemistry and a great number of reaction mechanisms are well understood. Most PLP enzymes have an active site lysine that forms an internal aldimine linkage with the cofactor in their holo form. Amino acids can attack the internal aldimine linkage, displacing the lysine and functionalizing the cofactor. Once the amino acid is bound, the cofactor acts as an electron sink enabling reactions at the α -position (racemization, decarboxylation, α -elimination/replacement, and transaminations) and at the β -position (elimination/replacement).

1.6. One-Carbon Metabolism

One-carbon metabolism in *S. enterica* provides precursors for the synthesis of a number of compounds: methionine, histidine, formyl-methionine, purines, methylated DNA, pantothenate, and thiamine [32]. One-carbon units are generated in two sequential metabolic steps: (1) in the conversion of serine to glycine, catalyzed by the enzyme serine hydroxymethyltransferase, GlyA (Fig. 1.6.A) and in the breakdown of glycine via the glycine

cleavage complex [33]. It is important to note that when *Escherichia coli* are grown using glucose as their sole carbon source, the demands for glycine and one-carbon units are equal, meaning the glycine cleavage reaction is not utilized under those conditions [32]. However, when glycine is present in the media or generated from the catabolism of threonine, the glycine cleavage complex is expressed and active [34]. In the cellular reaction shown below (Figure 1.6.B), tetrahydrofolate (THF) acts as a formyl carrier as 5,10-methylene-THF. Methylene-THF is oxidized to 10-formyl-THF for the synthesis of purines or reduced to methyl-THF for methionine biosynthesis.

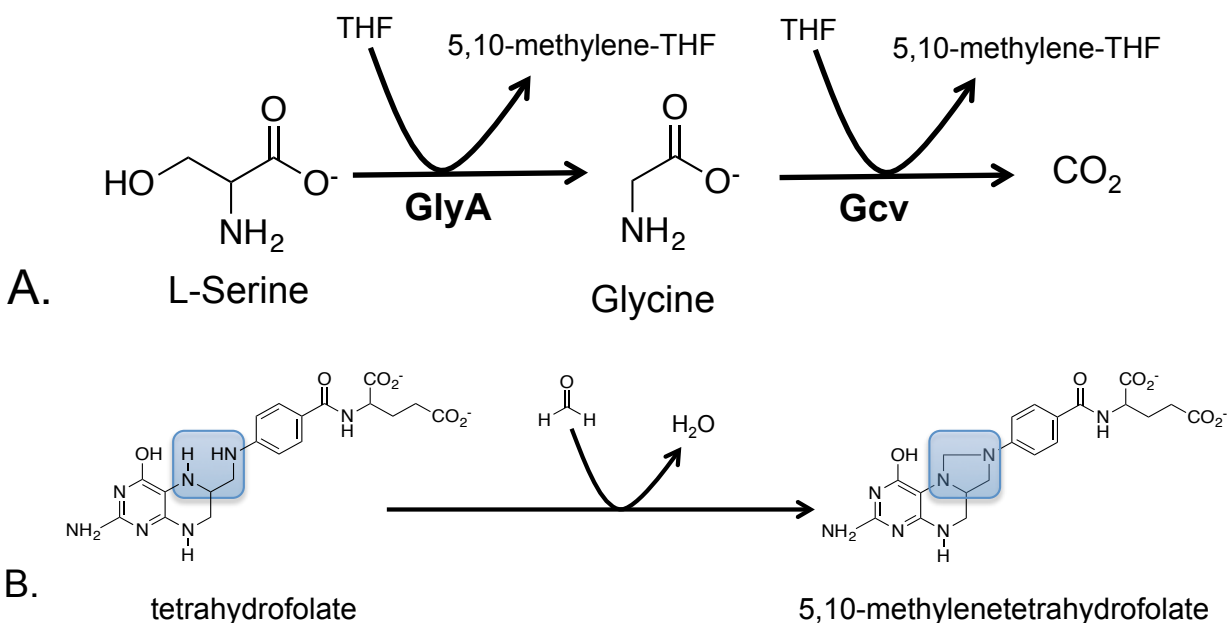


Figure 1.6. One-carbon unit generation. All the one-carbon units in the cell are generated in two sequential steps via serine hydroxymethyltransferase (GlyA) in the conversion of serine to glycine and the breakdown of glycine via the glycine cleavage complex (Gcv) (A). The formyl group abstracted from serine is added to tetrahydrofolate in between the nitrogens at the 5 and 10 positions of the cofactor shown above in the blue box (B) [33].

Given the disparate areas of metabolism where one-carbon units are utilized, one could imagine any perturbation to one-carbon metabolism would generate significant stress to the cell. The results in Chapter 3 show that strains lacking RidA have only 20% GlyA activity in crude extract from cells compared to wild type strains. It is remarkable to consider that these strains have only a slight growth defect when the only source for one-carbon units is so inhibited. This result highlights the tremendous ability of the cell to compensate for what, at first approximation, should cause a debilitating defect. This result alone emphasizes the complexity that is faced when unraveling *ridA* mutant phenotypes. The ability of the cell to compensate for metabolic defects has made isolation of inhibited enzymes difficult.

1.7. Dissertation Outline

This study began when the biochemical activity of RidA was just discovered, allowing for the generation of hypotheses to elucidate the *in vivo* role of RidA within the cell. This end was pursued using two complementary approaches: a targeted hypothesis-based inquiry and phenomenological phenotypic profiling. The results of these studies both gives proof for 2-AA accumulates in *ridA* mutant strains and significantly expands the number of enzymes inhibited in *ridA* strain. These enzymes are all PLP-enzymes, continuing the theme of *ridA* mutant phenotypes associated with PLP-enzyme inhibition.

The work in Chapter 2 began with the observation that RidA was an enamine deaminase, which allowed for the generation of a testable hypothesis: *ridA* strains will accumulate the inhibitory metabolite 2-AA. Alanine racemase (Alr) proved to be an excellent tool to probe the cell for the accumulation of 2-AA for the following reasons: (1) Alr has been extensively

characterized, (2) Alr is susceptible to 2-AA inhibition *in vitro*, and (3) straightforward analysis can give definitive proof of Alr exposure to 2-AA. The hypothesis that 2-AA accumulated in a *ridA* strain was supported by the isolation modified Alr from a *ridA* strain, this modification was consistent with 2-AA exposure. The modification of Alr correlated with reduced activity of the enzyme and gave direct evidence for 2-AA accumulation in *ridA* strains.

The work in Chapter 3 began with the observation made by a previous Downs Lab graduate student, Dr. Melissa Christopherson, that *ridA* mutant strains excrete pyruvate throughout exponential phase of growth while using glucose as a sole carbon source. Our model suggests that this phenotype is caused by the inhibition of a key enzyme(s) by 2-AA. Subsequent characterization showed that *ridA* strains are limited for CoA, which causes the pyruvate excretion. The CoA biosynthesis deficiency was the result of inhibition of the major one carbon unit enzyme, serine hydroxymethyltransferase. This study showed that RidA activity contributed to one carbon metabolism integrity, expanding our understanding of *ridA* mutant physiology. Furthermore, it identified serine hydroxymethyltransferase as an *in vivo* target for inhibition by 2-AA.

1.8 REFERENCES

1. Browne, B.A., A.I. Ramos, and D.M. Downs, *PurF-independent phosphoribosyl amine formation in yjgF mutants of Salmonella enterica utilizes the tryptophan biosynthetic enzyme complex anthranilate synthase-phosphoribosyltransferase*. J Bacteriol, 2006. **188**(19): p. 6786-92.

2. Lambrecht, J.A., B.A. Browne, and D.M. Downs, *Members of the YjgF/YER057c/UK114 family of proteins inhibit phosphoribosylamine synthesis in vitro*. J Biol Chem, 2010. **285**(45): p. 34401-7.
3. Lambrecht, J.A. and D.M. Downs, *Anthranilate Phosphoribosyl Transferase (TrpD) Generates Phosphoribosylamine for Thiamine Synthesis from Enamines and Phosphoribosyl Pyrophosphate*. ACS Chem Biol, 2012.
4. Enos-Berlage, J.L., M.J. Langendorf, and D.M. Downs, *Complex metabolic phenotypes caused by a mutation in yjgF, encoding a member of the highly conserved YER057c/YjgF family of proteins*. J Bacteriol, 1998. **180**(24): p. 6519-28.
5. Schmitz, G. and D.M. Downs, *Reduced transaminase B (IlvE) activity caused by the lack of yjgF is dependent on the status of threonine deaminase (IlvA) in Salmonella enterica serovar Typhimurium*. J Bacteriol, 2004. **186**(3): p. 803-10.
6. Christopherson, M.R., G.E. Schmitz, and D.M. Downs, *YjgF is required for isoleucine biosynthesis when Salmonella enterica is grown on pyruvate medium*. J Bacteriol, 2008. **190**(8): p. 3057-62.
7. Leitner-Dagan, Y., et al., *CHRD, a plant member of the evolutionarily conserved YjgF family, influences photosynthesis and chromoplastogenesis*. Planta, 2006. **225**(1): p. 89-102.
8. Oxelmark, E., et al., *Mmf1p, a novel yeast mitochondrial protein conserved throughout evolution and involved in maintenance of the mitochondrial genome*. Mol Cell Biol, 2000. **20**(20): p. 7784-97.

9. Andexer, J.N., et al., *Biosynthesis of the immunosuppressants FK506, FK520, and rapamycin involves a previously undescribed family of enzymes acting on chorismate*. Proc Natl Acad Sci U S A, 2011. **108**(12): p. 4776-81.
10. Burman, J.D., et al., *The crystal structure of Escherichia coli TdcF, a member of the highly conserved YjgF/YER057c/UK114 family*. BMC Struct Biol, 2007. **7**: p. 30.
11. Rappu, P., et al., *A role for a highly conserved protein of unknown function in regulation of Bacillus subtilis purA by the purine repressor*. J Bacteriol, 1999. **181**(12): p. 3810-5.
12. Ceciliani, F., et al., *The primary structure of UK114 tumor antigen*. FEBS Lett, 1996. **393**(2-3): p. 147-50.
13. Lambrecht, J.A., J.M. Flynn, and D.M. Downs, *Conserved YjgF protein family deaminates reactive enamine/imine intermediates of pyridoxal 5'-phosphate (PLP)-dependent enzyme reactions*. J Biol Chem, 2012. **287**(5): p. 3454-61.
14. Eliot, A.C. and J.F. Kirsch, *Pyridoxal phosphate enzymes: mechanistic, structural, and evolutionary considerations*. Annu Rev Biochem, 2004. **73**: p. 383-415.
15. Hillebrand, G.G., J.L. Dye, and C.H. Suelter, *Formation of an intermediate and its rate of conversion to pyruvate during the tryptophanase-catalyzed degradation of S-o-nitrophenyl-L-cysteine*. Biochemistry, 1979. **18**(9): p. 1751-5.
16. Walsh, C., et al., *Studies on the mechanism of action of the flavoenzyme lactate oxidase. Oxidation and elimination with beta-chlorolactate*. J Biol Chem, 1973. **248**(20): p. 7049-54.
17. Datta, P. and R. Bhadra, *Biodegradative threonine dehydratase. Reduction of ferricyanide by an intermediate of the enzyme-catalyzed reaction*. Eur J Biochem, 1978. **91**(2): p. 527-32.

18. Lambrecht, J.A., G.E. Schmitz, and D.M. Downs, *RidA proteins prevent metabolic damage inflicted by PLP-dependent dehydratases in all domains of life*. MBio, 2013. **4**(1): p. e00033-13.
19. Rabeh, W.M., S.S. Alguindigue, and P.F. Cook, *Mechanism of the addition half of the O-acetylserine sulphydrylase-A reaction*. Biochemistry, 2005. **44**(14): p. 5541-50.
20. Barends, T.R., M.F. Dunn, and I. Schlichting, *Tryptophan synthase, an allosteric molecular factory*. Curr Opin Chem Biol, 2008. **12**(5): p. 593-600.
21. Phillips, R.S., T.V. Demidkina, and N.G. Faleev, *Structure and mechanism of tryptophan indole-lyase and tyrosine phenol-lyase*. Biochim Biophys Acta, 2003. **1647**(1-2): p. 167-72.
22. Awano, N., et al., *Identification and functional analysis of Escherichia coli cysteine desulhydrases*. Appl Environ Microbiol, 2005. **71**(7): p. 4149-52.
23. Arfin, S.M. and D.A. Koziell, *Inhibition of growth of Salmonella typhimurium and of threonine deaminase and transaminase B by beta-chloroalanine*. J Bacteriol, 1971. **105**(2): p. 519-22.
24. Badet, B., D. Roise, and C.T. Walsh, *Inactivation of the dadB Salmonella typhimurium alanine racemase by D and L isomers of beta-substituted alanines: kinetics, stoichiometry, active site peptide sequencing, and reaction mechanism*. Biochemistry, 1984. **23**(22): p. 5188-94.
25. Esaki, N. and C.T. Walsh, *Biosynthetic alanine racemase of Salmonella typhimurium: purification and characterization of the enzyme encoded by the alr gene*. Biochemistry, 1986. **25**(11): p. 3261-7.

26. Roise, D., et al., *Inactivation of the Pseudomonas striata broad specificity amino acid racemase by D and L isomers of beta-substituted alanines: kinetics, stoichiometry, active site peptide, and mechanistic studies*. Biochemistry, 1984. **23**(22): p. 5195-201.
27. Ueno, H., J.J. Likos, and D.E. Metzler, *Chemistry of the inactivation of cytosolic aspartate aminotransferase by serine O-sulfate*. Biochemistry, 1982. **21**(18): p. 4387-93.
28. Kishore, G.M., *Mechanism-based inactivation of bacterial kynureninase by beta-substituted amino acids*. J Biol Chem, 1984. **259**(17): p. 10669-74.
29. Likos, J.J., et al., *A novel reaction of the coenzyme of glutamate decarboxylase with L-serine O-sulfate*. Biochemistry, 1982. **21**(18): p. 4377-86.
30. Tate, S.S., N.M. Relyea, and A. Meister, *Interaction of L-aspartate beta-decarboxylase with beta-chloro-L-alanine. Beta-elimination reaction and active-site labeling*. Biochemistry, 1969. **8**(12): p. 5016-21.
31. Wang, E.A., R. Kallen, and C. Walsh, *Mechanism-based inactivation of serine transhydroxymethylases by D-fluoroalanine and related amino acids*. J Biol Chem, 1981. **256**(13): p. 6917-26.
32. Matthews, R.G., *One-carbon metabolism, in Escherichia coli and Salmonella typhimurium Cellular and Molecular Biology*, F.C. Neidhardt, Editor 1996, American Society for Microbiology: Washington. p. 506-513.
33. Stauffer, G.V., *Biosynthesis of Serine, Glycine, and One-Carbon Units, in Escherichia coli and Salmonella typhimurium Cellular and Molecular Biology*, F.C. Neidhardt, Editor 1996, American Society for Microbiology: Washington. p. 506-513.
34. Stauffer, G.V., L.T. Stauffer, and M.D. Plamann, *The Salmonella typhimurium glycine cleavage enzyme system*. Mol Gen Genet, 1989. **220**(1): p. 154-6.

CHAPTER 2

In the Absence of RidA, Endogenous 2-Aminoacrylate Inactivates Alanine Racemases by Modifying the Pyridoxal 5'-Phosphate Cofactor

All of the work performed for this chapter was performed by myself with the exception of contract NMR spectroscopy and mass spectrometry. Much thanks go to Cameron Scarlett for performing mass spectral analysis and Mark Anderson for performing NMR analysis.

This Chapter comprises a manuscript accepted to the Journal of Bacteriology.

2.1 ABSTRACT

Members of the RidA (YjgF/YER057c/UK114) protein family are broadly conserved across the domains of life. *In vitro*, these proteins deaminate 3 or 4 carbon enamines that are generated as mechanistic intermediates of PLP-dependent serine threonine dehydratases. The three carbon enamine 2-aminoacrylate can inactivate some enzymes by forming a covalent adduct by a mechanism that has been well characterized *in vitro*. The biochemical activity of RidA suggested that the phenotypes of *ridA* mutant strains are caused by the accumulation of reactive enamine metabolites. The data herein show that in *ridA* mutant strains of *Salmonella enterica*, a stable 2-aminoacrylate/pyridoxal 5'-phosphate (2-AA/PLP) adduct forms on the biosynthetic alanine racemase, Alr, indicating the presence of 2-aminoacrylate *in vivo*. This study confirmed the deleterious effect of 2-aminoacrylate generated by metabolic enzymes and emphasized the need for RidA to quench this reactive metabolite.

2.2 INTRODUCTION

The RidA (previously the YjgF/YER057c/UK114) family of proteins is highly conserved and widely distributed in all domains of life [1-3]. Past studies in *S. enterica* and other organisms identified phenotypes that resulted from loss of RidA [2-7]. The diversity of phenotypes made it difficult to assign a unifying role for RidA. Results from numerous genetic and biochemical analyses led us to suggest that the role of RidA was to eliminate reactive metabolites that could inhibit key enzymes or catalyze anomalous chemical reactions [4, 7, 8]. This model was bolstered by the findings that in *ridA* strains of *S. enterica*, i) the activity of transaminase B (IlvE) was decreased by a post-translational mechanism [7] that depended on the dehydration of serine by threonine dehydratase IlvA [9], and ii) 2-aminocrotonate derived from threonine

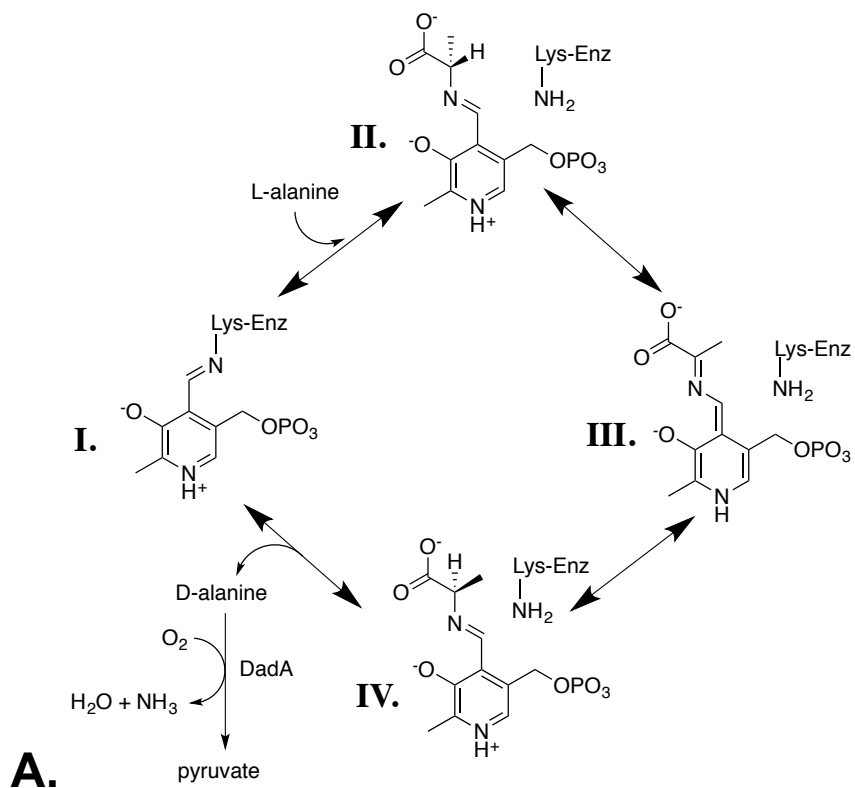
facilitated anomalous synthesis of the thiamine intermediate phosphoribosylamine by anthranilate phosphoribosyl transferase (TrpD) [1, 10].

RidA protein family members deaminate the 3 and 4 carbon enamines, 2-aminoacrylate (2-AA) and 2-aminocrotonate, respectively, *in vitro* [11]. These enamines are intermediates in the pyridoxal 5'-phosphate (PLP)-dependent mechanism of serine/threonine dehydratases (e.g., IlvA). The metabolites are unstable and are rapidly deaminated to ketoacids non-enzymatically in aqueous solution, even in the absence of RidA [12]. This nonenzymatic breakdown historically appeared to negate a need for enzymatic enamine deaminase activity.

Despite the rapid hydrolysis of the enamines in aqueous solution, the *in vitro* demonstration that RidA had deaminase activity suggests that enamine intermediates produced by cellular enzymes (e.g., serine/threonine deaminases) are relevant in the cellular environment. We hypothesized that if the role of RidA were to quench reactive enamines, cells lacking RidA would accumulate enamines. This hypothesis is supported by the *in vitro* demonstration that the activity of threonine dehydratase (IlvA), using serine as substrate, inactivated transaminase B (IlvE) in the absence of RidA [9]. The same study showed that a modified IlvE was isolated from a *ridA* mutant strain, but not from a wild-type strain. These data confirmed the role of RidA in protecting enzymes from post-translational modification and identified an enzyme responsible for generating a relevant reactive metabolite [9].

Certain β -substituted amino acids (e.g. serine *O*-sulfate and β -chloroalanine) can act as suicide substrates for certain PLP-enzymes. In the active site of these enzymes, these substrates are enzymatically converted to the RidA substrate, 2-AA. Once in the active site, 2-AA covalently modifies the active site thus rendering the enzyme inactive [13-18]. Two mechanisms for inactivation have been described, i) a 2-AA-PLP adduct formed as an external aldimine can

be attacked by a non-lysine nucleophilic residue in the active site [15, 17, 19, 20] or ii) the 2-AA attacks the PLP bound to the active-site lysine generating a 2-AA/PLP adduct that can be recovered as a pyruvate/PLP adduct after denaturing the protein (Figure 2.1.B) [16, 18, 21, 22]. The inhibitory nature of 2-AA as characterized in these *in vitro* reports suggested that 2-AA is a relevant reactive metabolite in strains lacking RidA.



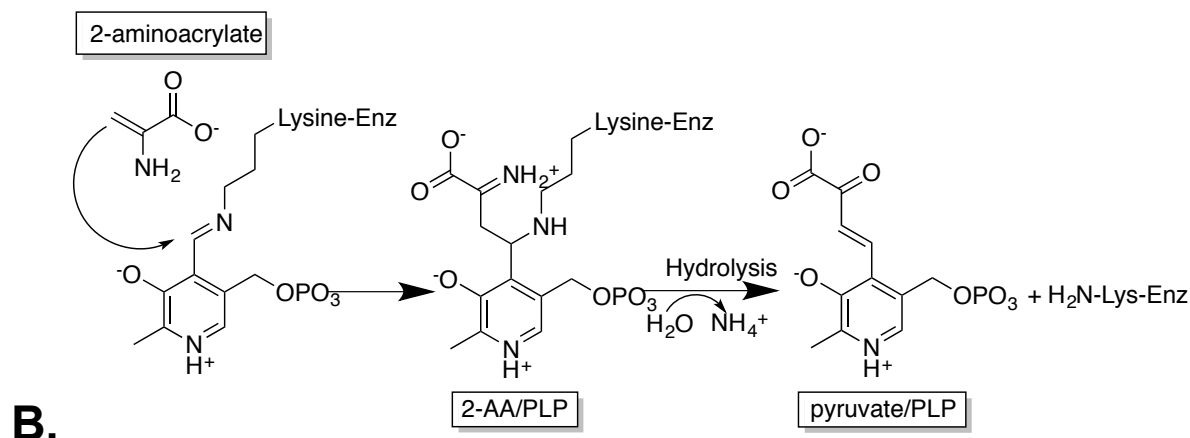


Figure 2.1. Catalytic mechanism of alanine racemase and mechanism of 2-aminoacrylate inhibition in Alr. (A) The catalytic mechanism of PLP-dependent alanine racemase has four states: (I) PLP cofactor is bound to the enzyme via an internal aldimine bond, (II) L-alanine attacks the aldimine linkage, displacing the lysine and forms an external aldimine, (III) the abstraction of the α -proton results in a quinonoid intermediate, (IV) the addition of the α -proton on the opposite side of the molecule results in the formation of D-alanine external aldimine which can be released to obtain (I) again. In L-alanine catabolism, D-alanine is oxidized via D-amino acid oxidase releasing ammonia and pyruvate. (B) 2-aminoacrylate (e.g. generated from β -chloroalanine) can attack the internal aldimine formed by the PLP cofactor bound to the active site lysine. The resulting enzyme is covalently modified and inactive due to the 2-aminoacrylate-modified PLP (2-AA/PLP). Upon base denaturation of the 2-aminoacrylate-modified enzyme, an adduct of pyridoxal 5'-phosphate and pyruvate (pyruvate/PLP) is released [14].

The current study was initiated to determine if 2-AA inactivation of PLP enzymes occurred *in vivo*, despite the short half-life of this enamine. To test this hypothesis, we chose to investigate alanine racemases in *S. enterica* with an emphasis on the biosynthetic enzyme, Alr. Inactivation of Alr by aminoacrylate via suicide substrates has been studied thoroughly *in vitro*

and occurred by the mechanism described above [14]. The data herein showed that, in the absence of RidA there is aminoacrylate-mediated inactivation of alanine racemase. To our knowledge this is the first report of the isolation of a PLP adduct formed by endogenously generated 2-aminoacrylate, and supports the hypothesis that the RidA family of proteins attenuates this enamine stress.

2.3 Materials and Methods

2.3.1. Bacterial strains, media, and chemicals.

Strains used in this study are derivatives of *Salmonella enterica* serovar Typhimurium LT2 and the genotypes are shown in Table 2.1. MudJ refers to the Mud1734 transposon [23]. An insertion-deletion of the *dadX* gene was generated by recombination methods described previously whereby the *dadX* gene was replaced by the *cat*⁺ gene from plasmid pKD3, which encodes chloramphenicol acetyltransferase [24]. A high-frequency general transducing mutant of bacteriophage P22 was used for transductional crosses required for strain construction [25]. Plasmid pJF2 is a derivative of pBAD24 [26], and contains a gene fusion of *alr* and the gene encoding the self-cleaving intein chitin-affinity tag. This fusion protein was functional and supported alanine racemase activity that could be measured prior to cleaving the tag.

Strain	Genotype
DM3480	<i>ridA3::MudJ</i>
DM9404	Wild type
DM13674	Wild type/pJF2
DM13675	<i>ridA3::MudJ/pJF2</i>
DM13756	<i>dadX::cat ridA3::MudJ</i>
DM13760	<i>dadX::cat</i>
DM14178	<i>alr::cat</i>
DM14179	<i>alr::cat ridA3::MudJ</i>
DM14180	<i>dadX::cat alr::kan</i>

TABLE 2.1. Bacterial Strains. MudJ refers to the Mud1734 transposon [23]. The plasmids are derivatives of pBAD24 [26].

Minimal medium was no-carbon E (NCE), or no-carbon no-nitrogen (NCN), supplemented with 1mM MgSO₄ [27] and 22 mM D-glucose. In the case of NCN, the nitrogen source was as indicated. Difco nutrient broth (NB; 8 g/L) with NaCl (5g/L) was used as a rich medium. Difco BiTek agar was added (15g/L) for solid medium. When required for plasmid maintenance, ampicillin was added to minimal and nutrient media at 15 and 150 mg L⁻¹, respectively. Unless noted, all chemicals and enzymes were purchased from Sigma-Aldrich Co. (St. Louis, MO).

2.3.2. Molecular biology - construction of pJF2.

The *alr* gene was amplified from *S. enterica* LT2 with primers JMF64 (5' TAGCATATGCAAGCGGCAACAGTCGT 3') and JMF65 (5' TAGCTCGAGATCAATATAC TTCATCGCCACCCT 3') using Herculase II Polymerase (Agilent Tech.). Following digestion with NdeI and XhoI, the gene fragment was cloned into pTYB2 (New England Biolabs,

IMPACT kit) to create pJF1, a plasmid containing a gene fusion of *alr* and the gene encoding the self-cleaving intein chitin-affinity tag. Plasmid pJF1 was cut with XbaI and PstI to excise the fragment containing *alr* and the affinity tag. The resulting fragment was cloned into plasmid pBAD24 [26] cut with NheI and PstI to create pJF2. The final construct was verified by sequencing the ligation junctions.

2.3.3. Alanine racemase assay - crude extract.

The assay for alanine racemase activity was adapted from an established protocol [28]. Briefly, 5-mL cultures were grown in minimal media to 0.8 OD₆₅₀ and harvested by centrifugation (8000 x g, 15 min). Cells pellets were resuspended in 0.9 ml of NaCl (145 mM) and permeablized by the addition of POPCULTURE reagent (Novagen) to a final concentration of 2% (v/v). Alanine racemase assay mixture contained: 10 to 810 µl of permeablized cells and glycine buffer (50 mM, pH 9.0) in a total volume of 1 mL; L-alanine was added to a final concentration of 100 mM to initiate the reaction. The mixture was incubated at 37°C, samples were removed at zero and 30 min and heated to 85°C for 5 min to terminate reactions. Resulting D-alanine concentrations were determined by conversion to pyruvate using D-amino acid oxidase (Sigma-Aldrich). The reaction for D-alanine determination contained: 900 µl of inactivated sample from above, D-amino acid oxidase (0.24 U), FAD⁺ (2.2 µM), bovine liver catalase (10 U) (Sigma-Aldrich) and glycine buffer (50 mM, pH 9.0) in a total volume of 1 mL. The reactions were continuously shaken and incubated at 37°C for 1 hour. To the 1mL reaction, 250 µL of 0.1% (w/v) dinitrophenol hydrazine in 2N HCL was added and allowed to react at room temperature for 15 min after which 1 mL of NaOH (1.5N) was added. After a 2 minute incubation at room temperature, absorbance at 520 nm was measured. A time course determined that D-alanine

concentrations increased linearly over 60 min. Absolute activity values varied between experiments done on different days, the ratio between strains was consistent. Cells were solubilized in sodium hydroxide (1.5 M), and the BCA Protein Assay (Thermo Scientific Pierce) was used to determine total cell protein using bovine serum albumin as a standard. Assays results were normalized to total cell protein. Data given are the mean and standard deviation of three biological replicates for strains DM13760 and DM13756 and two biological replicates for strains DM13674 and DM13675.

2.3.4. Alanine racemase assay - purified protein.

Racemization of D-alanine to L-alanine by pure protein was assayed by modifying a previously described protocol [21]. Briefly, the assay mixture contained 50 mM glycine pH 9, 1.2 mM NAD⁺, 20mM D-alanine, 0.1 units *Bacillus subtilis* L-alanine dehydrogenase (Sigma-Aldrich) and approximately 0.4 µg of Alr in a total volume of 105 µL. Reduction of NAD⁺ was monitored by the increase in absorbance at 340 nm. The extinction coefficient for NADH in 50 mM glycine (pH 9.0) was determined experimentally ($\epsilon=4000 \text{ AU M}^{-1} \text{ cm}^{-1}$) and used to calculate the rate of L-alanine production. Reactions were performed at room temperature and the specific activities are reported as $\mu\text{mol alanine min}^{-1} \text{ mg}^{-1}$. The BCA protein assay (Thermo Scientific Pierce) was used to measure protein concentration using bovine serum albumin as reference.

2.3.5. Protein purification.

Two liters of fresh minimal medium were inoculated with 50 mL of overnight cultures of strains containing pJF2 grown on minimal media shaking at 37°C. When the cultures reached an

OD₆₅₀ of 0.5, L-(+)-arabinose was added to 0.2% (w/v) final concentration to induce *alr* expression. Cells were harvested by centrifugation (15 min at 9,000 x g) when the OD₆₅₀ of the culture was between 2-2.5; resulting cell pellets were frozen at -80°C. Pellets were resuspended in 4-(2-hydroxyethyl)-1-piperazineethanesulfonic acid buffer (HEPES, 20 mM, pH 8.5) containing sodium chloride (100 mM), and cells were broken with a French Pressure cell (2 passes at 10342 kPa). After clarification by centrifugation (45 min at 48,000 x g), the supernatant was loaded onto to a chitin resin (5 mL) and protein purification proceeded as per manufacturer's instructions (New England Biolabs, IMPACT). After elution, protein was concentrated and dialyzed into 30 mM potassium phosphate buffer pH 8.3. Yields were approximately 1 mg Alr per liter of starting culture.

2.3.6. Characterization of cofactor content.

Cofactors bound to Alr were released from the protein as described elsewhere [16]. Briefly, KOH (30 mM final) was added to purified Alr (~2 mg/mL in 30mM potassium phosphate buffer, pH 8.3) and incubated at room temperature for 10 min. The protein was precipitated by adding potassium phosphate buffer (500 mM, pH 7.0) until the solution reached neutral pH or alternately by adding 10% trifluoroacetic acid until protein precipitate was formed. Precipitated protein was removed by centrifugation (3 min at 16,000 x g) and the cofactor content of the supernatant was analyzed by high performance liquid chromatography. The separations were performed on a Shimadzu HPLC equipped with a Luna 5m C18 (250 x 4.60 mm, 5 micron) (Phenomenex) using a 2-step isocratic method with a flow rate of 0.8 mL/min: 0-5 minutes, 100% buffer A (0.06% (v/v) trifluoroacetic acid), 5-18 minutes, methanol:buffer A (3:97). Between each run the column was washed for 10 min with methanol:buffer A (60:40).

The eluent was monitored at 305 nm using a photodiode array detector (Shimadzu SPD-M20A). Areas under the peaks were integrated using Shimadzu LabSolutions software (version 5.42). Authentic pyridoxal 5'-phosphate (>98% pure, Sigma-Aldrich) and 2-aminoacrylate-modified PLP (2-AA/PLP) served as standards. 2-AA/PLP (4-[2-methyl-3-hydroxy-5-(phosphooxymethyl)-4-pyridinyl]-2-oxo-3-butenoic acid) was synthesized as described [29], purified using HPLC and lyophilized. ¹H NMR was performed by the National Magnetic Resonance Facility at Madison on a 600.14 MHz Bruker DMX NMR spectrometer. The ¹H NMR spectrum of the synthesized compound contained the diagnostic peaks of the previously published spectrum for pyruvate/PLP [16] (H₂O:D₂O, 80:20 at pH 3.5): δ 2.624 (s), 5.037 (d, J=7.8 Hz), 7.525 (dd, J=238.8 Hz, J'=16.8 Hz), 8.075 (s); 4,4-dimethyl-4-silapentane-1-sulfonic acid (DSS) was used as an internal standard. The previously published extinction coefficient ($A_{\max} = 408 \text{ nm}$, $\epsilon = 8000 \text{ cm}^{-1} \text{ M}^{-1}$) of AA-PLP was used to determine the concentration at pH 7.0 [21]. Data given are triplicate measurements of a representative purification represented as mean \pm standard deviation.

2.3.7. Mass spectroscopy of cofactor.

Cofactors were released and separated as described above. Eluent corresponding to pyruvate/PLP was collected and twice lyophilized to remove trifluoroacetic acid. Samples were analyzed at the University of Wisconsin School of Pharmacy Mass Spectrometry Facility. Samples were diluted in 50% acetonitrile and analyzed using ESI infusion mass spectrometry in the negative ion mode with a Bruker Maxis 4G UHR-ToF mass spectrometer.

2.4. RESULTS and DISCUSSION

2.4.1. *ridA* mutant strains are compromised in utilization of L-alanine as a nitrogen source.

Bacterial alanine racemases are PLP-containing enzymes that catalyze the racemization of L-alanine to D-alanine and vice versa by the mechanism shown in Figure 2.1.A. Like *E. coli*, the *S. enterica* genome encodes both a biosynthetic and a catabolic alanine racemase, Alr and DadX respectively [30]. Although the proteins are homologous, their roles *in vivo* are distinct due to the differing regulation of their expression. The former (Alr) is required to convert L-alanine to D-alanine, an essential precursor of the peptidoglycan layer in the cell wall and is constitutively expressed at a low level [31]. In contrast, L-alanine can be used by *S. enterica* as sole nitrogen source by a pathway that requires the catabolic alanine racemase, DadX (Figure 2.1.A) expressed at significantly higher levels than Alr.

Growth curves were performed using L-alanine as the sole nitrogen source (Fig. 2.2.A). As expected, growth of strains containing a deletion of *alr* were similar to wild type strains while strains containing a deletion of *dadX* were unable to grow. *ridA* mutant strains grew poorly using L-alanine as a nitrogen source, displaying a rate and final density that was midway between wild type and a *dadX* mutant. *ridA* strains showed a similar defect when L-alanine was provided as sole carbon source (data not shown). The *ridA* mutants did not have a defect when utilizing D-alanine as the sole nitrogen source, a growth condition that circumvented the need for alanine racemase activity (Figure 2.2.B). These results suggested that alanine racemase activity contributed by DadX was compromised in a *ridA* strain, but did not address an impact of RidA on the activity of Alr.

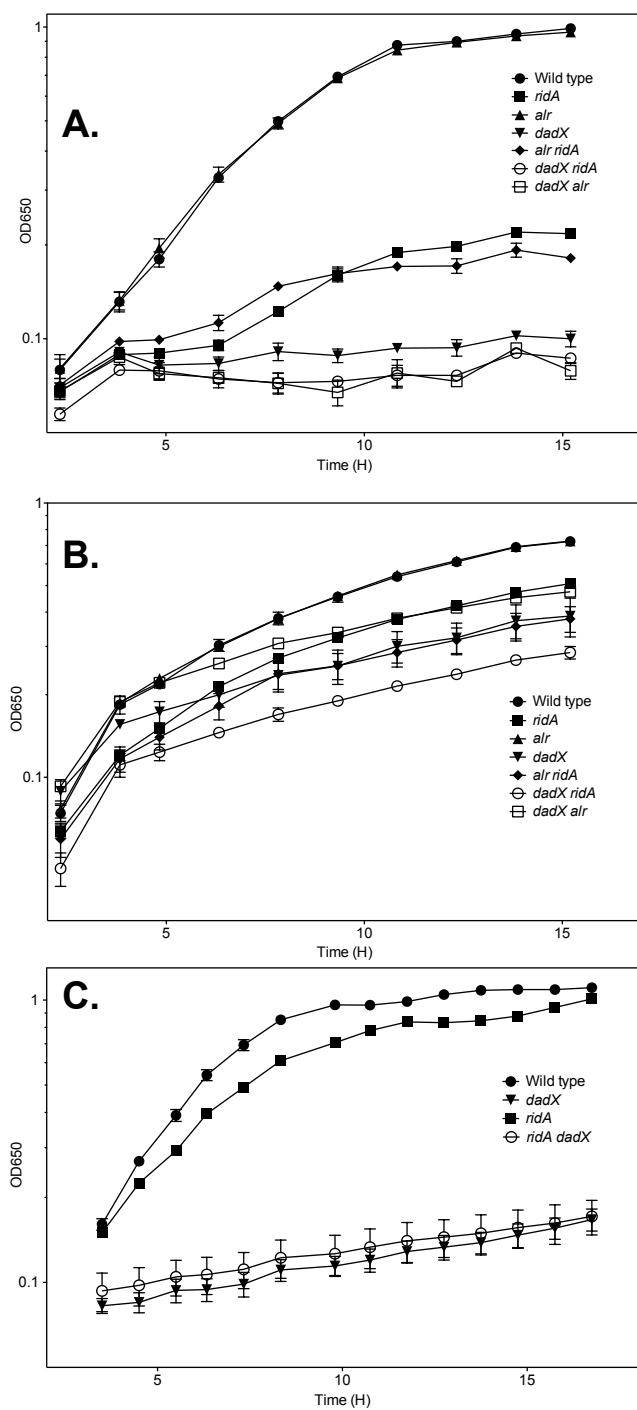


Figure 2.2. *ridA* mutants are compromised in the utilization of L-alanine as a nitrogen source. Growth curves were performed by monitoring optical density (OD) at 650 nm. Indicated strains were growth in minimal nitrogen-free medium (NCN) supplemented with L-alanine (5mM) (A),

D-alanine (5mM) (B), and L-alanine (5mM) with isoleucine (0.3mM) (C). Data represent growth curves performed in triplicate, given values are mean \pm standard deviation, many points of wild type and *alr* strains are overlapping in curves.

2.4.2. Alanine racemase activity is compromised in *ridA* mutant strains.

Several relevant strains were grown in minimal medium, the cells were permeablized and alanine racemase activity assayed. The effect that the lack of RidA had on each isozyme was addressed by assaying isogenic strains expressing one or the other racemase (Table 2.2). In strains with a functional DadX and lacking RidA, alanine racemase activity was \sim 70% of that measured in an isogenic strain with a functional RidA. These data allowed the conclusion that DadX was compromised in the absence of RidA. In the strains lacking DadX, the low level of racemase activity contributed by Alr made it difficult to address whether Alr was similarly compromised in the absence of RidA.

Strain	Genotype	Alanine racemase specific activity (nmol D-ala min ⁻¹ mg ⁻¹)	Percent of wild type
DM9404	Wild type	61.6 ± 7.4	
DM3480	<i>ridA</i>	42.7 ± 2.5	69
DM14178	<i>alr</i>	66.0 ± 1.5	107
DM13760	<i>dadX</i>	2.3 ± 0.2	3.7
DM14179	<i>alr ridA</i>	41.0 ± 1.6	66
DM13756	<i>dadX ridA</i>	2.1 ± 0.3	3.5
DM14180	<i>alr dadX</i>	1.2 ± 0.2	2.0

TABLE 2.2. Alanine racemase activity in permeabilized cells. Alanine racemase activity was assayed in permeabilized cells as described in the Materials and Methods. Shown are averages and standard deviations for biological triplicates.

Alr was expressed as an intein-chitin binding domain fusion to overcome the difficulties associated with the low level of activity from chromosomally encoded Alr. When the fusion protein was overexpressed, alanine racemase activity in a *ridA* strain was 62% of that found in the wild-type strain (371 ± 28 and 230 ± 36 nmol D-alanine min⁻¹ mg⁻¹, respectively). The difference between the racemase activity in a *ridA* and wildtype strain indicated the status of RidA affected the activity of Alr in addition to that of DadX.

2.4.3. Isoleucine addition corrects growth defect of RidA deficient strains.

Previous work showed that an activity of the biosynthetic serine/threonine dehydratase, IlvA, caused partial inactivation of the branched chain transaminase, IlvE in a *ridA* strain [7]. To address if IlvA activity was involved in modulating the activity of alanine racemase in the absence of RidA, isoleucine was added to the medium. The addition of isoleucine corrected the growth defect of a *ridA* strain using L-alanine as a nitrogen source, but had no effect on the

growth of the *dadX* strain (Fig. 2.2C). Isoleucine decreases IlvA activity through a feedback inhibition mechanism, and this result suggested that IlvA activity was required for inactivation of the alanine racemases in strains lacking RidA.

2.4.4. Alr protein purified from *ridA* cells is modified.

The above data were consistent with a post-translational modification, derived from an intermediate in the dehydratase reaction of IlvA, contributing to the decreased racemase activity in a *ridA* strain. In one scenario, the accumulation of endogenous 2-AA in *ridA* strains would inactivate Alr via the 2-AA/PLP adduct previously characterized *in vitro* (Fig. 2.1B). If this were the case, a pyruvate/PLP adduct would be released from Alr when the protein was denatured [14, 21]. Alr was overexpressed and purified to >95% homogeneity from *ridA*⁺ and *ridA* strains grown in minimal medium. The two Alr protein samples, and an additional control sample, were denatured and the released cofactor(s) was separated by HPLC. The protein samples were, i) Alr purified from wild-type (*ridA*⁺) genetic background, ii) Alr purified from wild-type (*ridA*⁺) background and partially inactivated by incubation with β -chloroalanine, and iii) Alr purified from a *ridA* strain. The cofactor content of each protein sample is depicted in the HPLC chromatograms shown in Figure 2.3. When monitored at 305 nm, two peaks were observed. The first, larger peak had a retention time of 10.3 min and was present in all three samples. The second peak was significantly smaller, had a retention time of 14.2 min and was present only in the sample purified from a *ridA* strain and the sample treated with β -chloroalanine. The sample derived from the wild-type strain had no detectable absorbance (≤ 500 AU) at 305nm between 13.5 and 14.5 min.

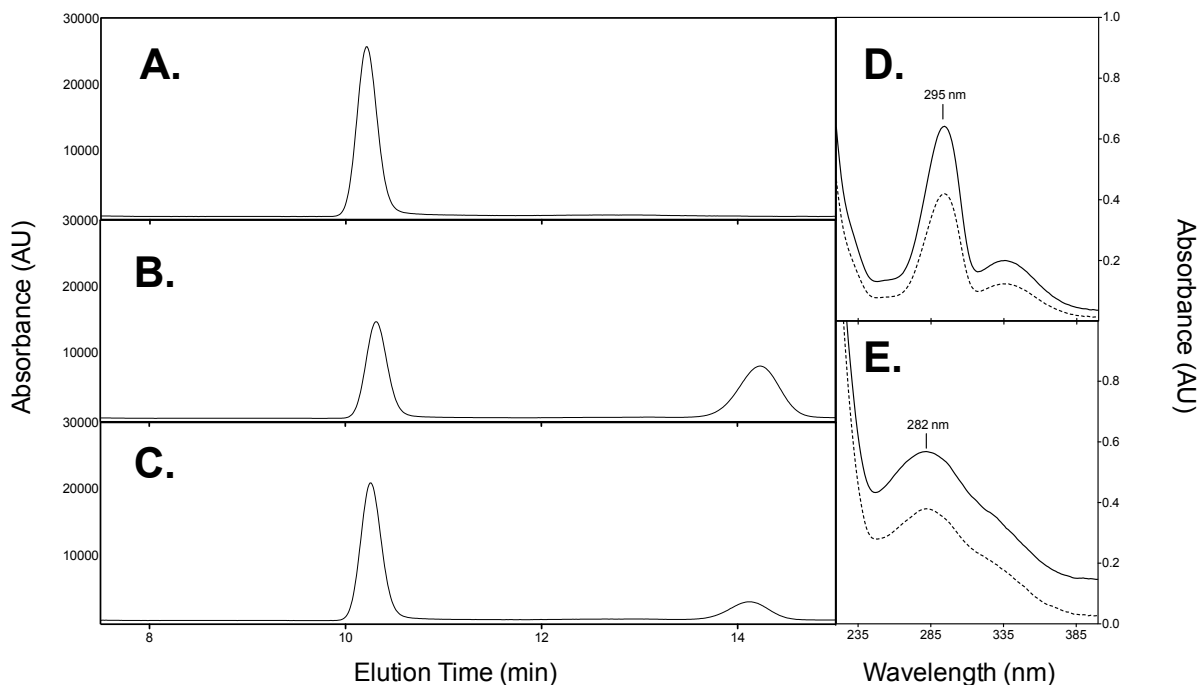


Figure 2.3. Alr isolated from *ridA* strain contains multiple cofactors. Protein isolated from wild type (A), wild type protein partially treated with β -chloroalanine (B) and protein isolated from *ridA* (C) were denatured to release the cofactor and protein-free supernatant was analyzed by HPLC. The UV/Vis spectra of authentic PLP (D) and pyruvate/PLP (E) were compared to spectra from the peaks of *ridA*-isolated Alr at pH 2. Authentic species (—) and *ridA*-isolated (---) spectra compare.

The similarity between the chromatograph of the sample treated with β -chloroalanine and the sample from a *ridA* strain suggested the second peak was the pyruvate/PLP adduct derived from a 2-AA/PLP during base denaturation of the protein (Figure 2.1) [14, 16, 21]. Retention time, co-injection of authentic compounds, and UV-vis spectra (Figure 2.3.D and E) suggested the peak eluting at 10.3 min was PLP and the peak eluting at 14.2 min was a pyruvate/PLP adduct. This assignment was confirmed by mass spectrometry. The eluant from the peak at 14.2

min in both the β -chloroalanine treated Alr and *ridA*-isolated Alr contained the MS signatures of the synthesized adduct (Figure 2.4).

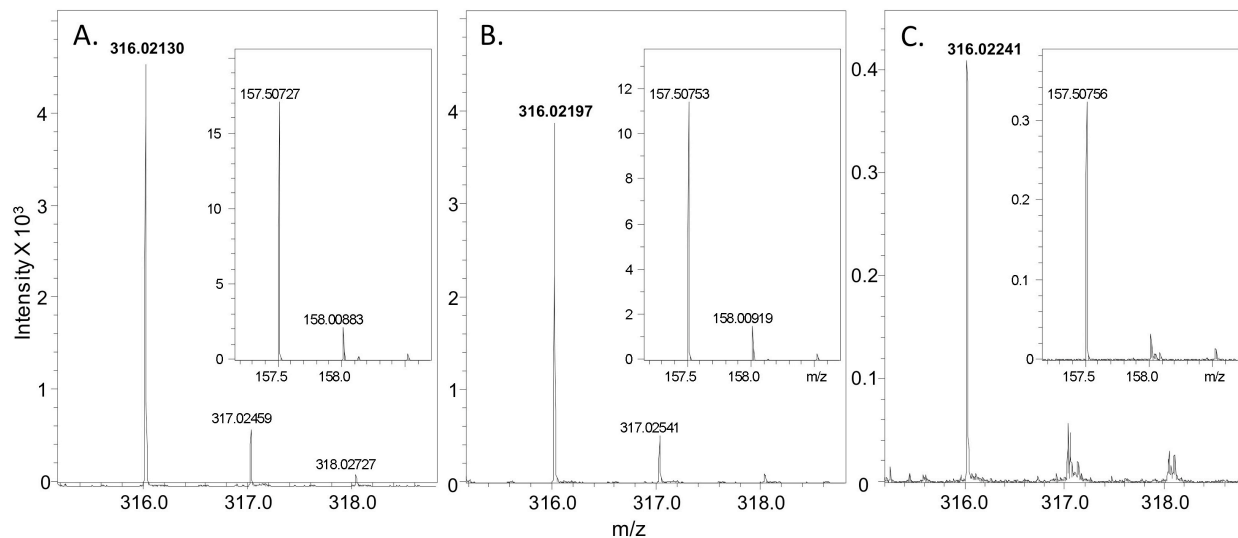


Figure 2.4. Alr isolated from *ridA* strain contains 2-aminoacrylate-modified cofactor.

Authentic pyruvate/PLP (A), the 14.2 min HPLC eluant from denatured Alr treated β -chloroalanine (B), and the 14.2 min HPLC eluant from denatured Alr isolated from *ridA* mutant strain (C) were subjected to mass spectral analysis. All contained a major species with an m/z 316.02278 (± 5 ppm) corresponding to the mass of pyruvate/PLP and another species (inset) with an m/z 157.50699 (± 5 ppm) corresponding to the charged (-2) molecule.

The cofactor isolated from the Alr from wild-type and *ridA* strains was quantified by integrating the area under each peak shown in Figure 2.3. The total amount of cofactor isolated from each sample was similar (19.61 and 18.09 nmol mg⁻¹, respectively). These numbers indicated that the concentration of PLP-populated enzyme was not significantly different between the two samples. However, a reproducible difference in the composition of cofactor was measured in the samples from the wild-type (19.61 \pm 0.14 nmol mg⁻¹, PLP) and *ridA* (15.44 \pm

0.05 and 2.65 ± 0.07 nmol mg⁻¹, PLP and pyruvate/PLP respectively) strains. Further, the pyruvate/PLP accounted for approximately 15% of the cofactor released from the Alr sample isolated from the *ridA* mutant strain. Activity levels of the two Alr protein samples were consistent with these data. First, the Alr protein isolated from the strain lacking RidA was ~15% less active than the protein purified from wild type (2.19 ± 0.06 and 2.56 ± 0.16 μmol L-alanine min⁻¹ mg⁻¹, respectively). Furthermore, the addition of PLP to the activity assay increased the specific activity of both preparations proportionally (2.56 ± 0.11 and 2.91 ± 0.10 μmol L-alanine min⁻¹ mg⁻¹ for protein from *ridA* and wild type, respectively). The ~15% difference in activity between the two protein samples was determined to be statistically significant ($p=0.021$ and $p=0.014$), although it was not as extensive as the ~40% difference in Alr activity measured in crude extracts. The disparity between the ratio of activities measured in crude extract versus with purified protein may suggest that the 2-AA-modified protein is unstable *in vivo*, or lost in the purification. Taken together, these data indicate a modification generated by endogenous 2-AA exposure contributed to the decreased activity of Alr in a strain lacking RidA.

2.5. CONCLUSIONS

In bacteria and other organisms there are multiple PLP-dependent enzymes known to generate 2-AA as part of the biochemical mechanisms: serine/threonine dehydratases [29, 32], cysteine desulfhydrases [33], tryptophanase [34] and tryptophan synthase [35], among others. While the reactivity of aminoacrylate has been emphasized by studies *in vitro*, the potential for this, and similar enamines, to cause significant damage *in vivo* has only recently come to light based on work with RidA [9-11]. The significance of 2-AA as a metabolic stressor was not appreciated because of the short half-life of this metabolite in aqueous solution (~1.5 seconds)

and the resulting expectation that it would not persist in the cellular environment [12]. The demonstration that RidA was a 2-aminoacrylate deaminase, coupled with the multiple phenotypes of a *ridA* strain, suggested that endogenously generated 2-AA could pose a significant risk *in vivo*. However, rigorous evidence of 2-AA-induced damage *in vivo* and the mechanism by which it occurs were lacking. This study was initiated to define the consequences of 2-AA accumulation in the cell at a molecular level.

This work made use of the molecular characteristics of an adduct formed by exposing Alr to 2-AA *in vitro*. The isolation of a pyruvate/PLP adduct from a cellular protein provided the first direct evidence that 2-AA accumulates *in vivo*. Despite the presence of the same modification on Alr protein that was inactivated *in vivo* or *in vitro*, the difference between the two mechanisms is worth noting. Inactivation of the enzyme *in vitro* required the formation of 2-AA from β -chloroalanine in the active site of Alr [14, 16, 21]. In contrast, in this study the source of the 2-AA was from a metabolic enzyme(s) in the cell. A recent report showed that 2-AA generated by one enzyme, threonine dehydratase (IlvA), was able to enter and inactivate a second enzyme, transaminase B (IlvE) *in vitro* [9]. The relevant study provided evidence the same mechanism occurred *in vivo*, consistent with the results herein indicating endogenously generated reactive 2-AA can modify proteins. The covalent PLP adduct formed on IlvE, both *in vivo* and *in vitro* was distinct from the one reported here [9].

PLP-dependent enzymes in addition to transaminase B and alanine racemases are likely to be inhibited by 2-AA-mediated inactivation in *ridA* mutants. With the described examples, two different PLP adducts have been identified, both of which were previously characterized *in vitro*. It remains to be seen whether additional distinct 2-AA generated modifications exist *in vivo*. Future studies to identify the breadth of the enzymes affected in *ridA* strains have potential

to provide insights into characteristics that make an enzyme susceptible to modification (i.e. active site configuration) via cellular 2-AA.

In combination with other reports, the data herein emphasize that endogenously generated 2-AA persists free in the cellular milieu long enough to enter distinct active sites. To reconcile this conclusion with the characteristic half-life of enamines in aqueous solutions [12] requires that our understanding of the cellular milieu be reassessed. Genetic dissection of this system will complement biochemical/biophysical efforts that continue to define characteristics the cellular environment.

2.6. REFERENCES

1. Lambrecht, J.A. and D.M. Downs, *Anthranilate Phosphoribosyl Transferase (TrpD) Generates Phosphoribosylamine for Thiamine Synthesis from Enamines and Phosphoribosyl Pyrophosphate*. ACS Chem Biol, 2012.
2. Leitner-Dagan, Y., et al., *CHRD, a plant member of the evolutionarily conserved YjgF family, influences photosynthesis and chromoplastogenesis*. Planta, 2006. **225**(1): p. 89-102.
3. Oxelmark, E., et al., *Mmf1p, a novel yeast mitochondrial protein conserved throughout evolution and involved in maintenance of the mitochondrial genome*. Mol Cell Biol, 2000. **20**(20): p. 7784-97.
4. Christopherson, M.R., G.E. Schmitz, and D.M. Downs, *YjgF is required for isoleucine biosynthesis when Salmonella enterica is grown on pyruvate medium*. J Bacteriol, 2008. **190**(8): p. 3057-62.

5. Enos-Berlage, J.L., M.J. Langendorf, and D.M. Downs, *Complex metabolic phenotypes caused by a mutation in yjgF, encoding a member of the highly conserved YER057c/YjgF family of proteins*. J Bacteriol, 1998. **180**(24): p. 6519-28.
6. Kim, J.M., H. Yoshikawa, and K. Shirahige, *A member of the YER057c/yjgF/Uk114 family links isoleucine biosynthesis and intact mitochondria maintenance in Saccharomyces cerevisiae*. Genes Cells, 2001. **6**(6): p. 507-17.
7. Schmitz, G. and D.M. Downs, *Reduced transaminase B (IlvE) activity caused by the lack of yjgF is dependent on the status of threonine deaminase (IlvA) in Salmonella enterica serovar Typhimurium*. J Bacteriol, 2004. **186**(3): p. 803-10.
8. Browne, B.A., A.I. Ramos, and D.M. Downs, *PurF-independent phosphoribosyl amine formation in yjgF mutants of Salmonella enterica utilizes the tryptophan biosynthetic enzyme complex anthranilate synthase-phosphoribosyltransferase*. J Bacteriol, 2006. **188**(19): p. 6786-92.
9. Lambrecht, J.A., G.E. Schmitz, and D.M. Downs, *RidA proteins prevent metabolic damage inflicted by PLP-dependent dehydratases in all domains of life*. MBio, 2013. **4**(1): p. e00033-13.
10. Lambrecht, J.A., B.A. Browne, and D.M. Downs, *Members of the YjgF/YER057c/UK114 family of proteins inhibit phosphoribosylamine synthesis in vitro*. J Biol Chem, 2010. **285**(45): p. 34401-7.
11. Lambrecht, J.A., J.M. Flynn, and D.M. Downs, *Conserved YjgF protein family deaminates reactive enamine/imine intermediates of pyridoxal 5'-phosphate (PLP)-dependent enzyme reactions*. J Biol Chem, 2012. **287**(5): p. 3454-61.

12. Hillebrand, G.G., J.L. Dye, and C.H. Suelter, *Formation of an intermediate and its rate of conversion to pyruvate during the tryptophanase-catalyzed degradation of S-o-nitrophenyl-L-cysteine*. *Biochemistry*, 1979. **18**(9): p. 1751-5.
13. Arfin, S.M. and D.A. Koziell, *Inhibition of growth of Salmonella typhimurium and of threonine deaminase and transaminase B by beta-chloroalanine*. *J Bacteriol*, 1971. **105**(2): p. 519-22.
14. Esaki, N. and C.T. Walsh, *Biosynthetic alanine racemase of Salmonella typhimurium: purification and characterization of the enzyme encoded by the alr gene*. *Biochemistry*, 1986. **25**(11): p. 3261-7.
15. Kishore, G.M., *Mechanism-based inactivation of bacterial kynureninase by beta-substituted amino acids*. *J Biol Chem*, 1984. **259**(17): p. 10669-74.
16. Likos, J.J., et al., *A novel reaction of the coenzyme of glutamate decarboxylase with L-serine O-sulfate*. *Biochemistry*, 1982. **21**(18): p. 4377-86.
17. Relyea, N.M., S.S. Tate, and A. Meister, *Affinity labeling of the active center of L-aspartate-beta-decarboxylase with beta-chloro-L-alanine*. *J Biol Chem*, 1974. **249**(5): p. 1519-24.
18. Roise, D., et al., *Inactivation of the Pseudomonas striata broad specificity amino acid racemase by D and L isomers of beta-substituted alanines: kinetics, stoichiometry, active site peptide, and mechanistic studies*. *Biochemistry*, 1984. **23**(22): p. 5195-201.
19. Rando, R.R. and J. De Mairena, *Propargyl amine-induced irreversible inhibition of non-flavin-linked amine*. *Biochem Pharmacol*, 1974. **23**(2): p. 463-7.

20. Wang, E.A. and C. Walsh, *Characteristics of beta, beta-difluoroalanine and beta, beta, beta-trifluoroalanine as suicide substrates for Escherichia coli B alanine racemase*. *Biochemistry*, 1981. **20**(26): p. 7539-46.
21. Badet, B., D. Roise, and C.T. Walsh, *Inactivation of the dadB Salmonella typhimurium alanine racemase by D and L isomers of beta-substituted alanines: kinetics, stoichiometry, active site peptide sequencing, and reaction mechanism*. *Biochemistry*, 1984. **23**(22): p. 5188-94.
22. Ueno, H., J.J. Likos, and D.E. Metzler, *Chemistry of the inactivation of cytosolic aspartate aminotransferase by serine O-sulfate*. *Biochemistry*, 1982. **21**(18): p. 4387-93.
23. Castilho, B.A., P. Olfson, and M.J. Casadaban, *Plasmid insertion mutagenesis and lac gene fusion with mini-mu bacteriophage transposons*. *J Bacteriol*, 1984. **158**(2): p. 488-95.
24. Datsenko, K.A. and B.L. Wanner, *One-step inactivation of chromosomal genes in Escherichia coli K-12 using PCR products*. *Proc Natl Acad Sci U S A*, 2000. **97**(12): p. 6640-5.
25. Schmieger, H., *Phage P22-mutants with increased or decreased transduction abilities*. *Mol Gen Genet*, 1972. **119**(1): p. 75-88.
26. Guzman, L.M., et al., *Tight regulation, modulation, and high-level expression by vectors containing the arabinose PBAD promoter*. *J Bacteriol*, 1995. **177**(14): p. 4121-30.
27. Davis, R.W., D. Botstein, and J. R. Roth, *Advanced bacterial genetics*. 1980, Cold Spring Harbor, N.Y.: Cold Spring Harbor Laboratory.
28. Wild, J., et al., *Identification of the dadX gene coding for the predominant isozyme of alanine racemase in Escherichia coli K12*. *Mol Gen Genet*, 1985. **198**(2): p. 315-22.

29. Schnackerz, K.D., et al., *Mechanism of action of D-serine dehydratase. Identification of a transient intermediate*. *Biochemistry*, 1979. **18**(16): p. 3557-63.
30. Wasserman, S.A., C.T. Walsh, and D. Botstein, *Two alanine racemase genes in Salmonella typhimurium that differ in structure and function*. *J Bacteriol*, 1983. **153**(3): p. 1439-50.
31. Lambert, M.P. and F.C. Neuhaus, *Factors affecting the level of alanine racemase in Escherichia coli*. *J Bacteriol*, 1972. **109**(3): p. 1156-61.
32. Zhao, Z. and H. Liu, *A quantum mechanical/molecular mechanical study on the catalysis of the pyridoxal 5'-phosphate-dependent enzyme L-serine dehydratase*. *J Phys Chem B*, 2008. **112**(41): p. 13091-100.
33. Bharath, S.R., et al., *Structural and mutational studies on substrate specificity and catalysis of Salmonella typhimurium D-cysteine desulphydrase*. *PLoS One*, 2012. **7**(5): p. e36267.
34. Phillips, R.S., T.V. Demidkina, and N.G. Faleev, *Structure and mechanism of tryptophan indole-lyase and tyrosine phenol-lyase*. *Biochim Biophys Acta*, 2003. **1647**(1-2): p. 167-72.
35. Barends, T.R., M.F. Dunn, and I. Schlichting, *Tryptophan synthase, an allosteric molecular factory*. *Curr Opin Chem Biol*, 2008. **12**(5): p. 593-600.

CHAPTER 3

Decreased coenzyme A levels in *ridA* mutant strains of *Salmonella enterica* result from inactivated serine hydroxymethyltransferase

Acknowledgements: I performed the work in this chapter in collaboration with Melissa Christopherson; Melissa discovered the pyruvate accumulation phenotype in *ridA* strains and provided all the results presented in section 3.4.1.

This Chapter is a stand alone manuscript in final stages of preparation for submission.

3.1. ABSTRACT

The RidA/Yer057/UK114 family of proteins is well represented across the domains of life and recent work has defined both an *in vitro* activity and an *in vivo* role for RidA. RidA protein has enamine deaminase activity, and in its absence the reactive 2-aminoacrylate accumulates and inactivates certain pyridoxal 5'-phosphate (PLP)-containing enzymes in *Salmonella enterica*. The conservation of RidA across all domains of life suggests that 2-AA is a ubiquitous cellular stressor generated in central metabolism. Phenotypically, strains of *S. enterica* that lack RidA accumulated significantly more pyruvate in the growth medium than wild-type strains. Here we dissected this *ridA* mutant phenotype and showed it was an indirect consequence of damage to serine hydroxymethyltransferase (GlyA; E.C. 2.1.2.1). The results here identify a third PLP-enzyme as a target of enamine stress in *S. enterica*. Furthermore, this study found that a metabolic defect of a *ridA* strain can be generated by a perturbation that is relayed through the metabolic network, ultimately generating a detectable metabolic phenotype.

3.2. INTRODUCTION

The RidA/Yer057/UK114 family of proteins is highly conserved, with representative members throughout all domains of life [1-3]. RidA had enamine deaminase activity *in vitro*, where it accelerated the hydrolysis of 3 and 4 carbon enamine metabolites generated in the reaction mechanism of pyridoxal 5'-phosphate (PLP)-dependent dehydratases [2]. 2-Aminoacrylate (2-AA), a serine derived enamine, is generated in a number of biosynthetic and catabolic reactions [4-7], and is a known *in vitro* inhibitor of a number of PLP-containing enzymes [8-13]. Despite its reactivity *in vitro*, prior to characterization of RidA, 2-AA was not considered physiologically significant due to its short half-life in aqueous solutions. Recent

results showed that the removal of RidA from strains of *S. enterica* resulted in 2-AA-mediated inactivation of PLP-containing enzymes alanine racemase (Alr) and transaminase B (IlvE) [14]. Those studies established that the cellular half-life of 2-AA is long enough to allow irreversible damage of some cellular components. Based on a combination of *in vivo* and *in vitro* results we proposed that at least one role of RidA family members is to minimize levels of free 2-aminoacrylate (2-AA) in a cell and prevent damage caused by this reactive metabolite [2, 15, 16]. The broad conservation of the RidA family suggests that this metabolic stress is an unavoidable consequence of some PLP-dependent reactions and that the RidA protein family provides one solution to this problem.

Past work identified a variety of phenotypes of *ridA* mutants in *S. enterica* and other organisms [15-18]. The identification of a biochemical function for the protein family suggested that each phenotype might be attributed to the inactivation of one or more PLP-dependent enzymes. Thus, determining the causation of the observed phenotypes provides a means to identify cellular enzymes that generated 2-AA, and the enzymes that were inactivated this stressor. Precedent suggests that in the absence of RidA an accumulating stressor (*e.g.*, 2-AA) inactivates some percentage of the cellular PLP-dependent enzymes. In this scenario two types of phenotypes can result: (1) direct phenotypes, whereby the phenotype is a direct consequence of enzyme activity, and (2) indirect phenotypes, whereby the phenotype is an indirect effect of perturbations of the metabolic network. In the latter case, the causative defect may not be obvious from the detected phenotype. Based on the *in vitro* and *in vivo* work with RidA, our hypothesis is that in each case the target enzyme(s) will be PLP-dependent and the inactivation will be caused by a 2-AA generated adduct on the protein.

This study was initiated to identify the compromised enzyme in a *ridA* mutant that was

responsible for the increased accumulation of pyruvate in the growth medium when glucose was the sole carbon source. Nutritional and genetic approaches revealed that an enzyme in one-carbon metabolism, serine hydroxymethyltransferase, GlyA, was partially inactivated in a *ridA* strain, which indirectly resulted in the accumulation of pyruvate in the medium. Together the data herein expand our understanding of the phenotypic implications of perturbing the metabolic network and identify a third target for the 2-AA that accumulates in *ridA* mutant strains of *S. enterica*.

3.3. MATERIALS and METHODS

3.3.1. Bacterial strains, media, and chemicals.

All strains used in this study are derivatives of *S. enterica* serovar Typhimurium LT2 and are listed with their genotypes in Table 3.1. Minimal medium was no-carbon E (NCE) supplemented with 1 mM MgSO₄ [19] and 11 mM D-glucose. The following supplements were added where specified: 2-ketoisovalerate (100 μM), 2-ketopantoate (100 μM), β-alanine (100 μM), pantothenate (100 μM), glycine (670 μM) and isoleucine (300 μM). Difco nutrient broth (8 g/L) with NaCl (5 g/L) was used as a rich medium. Difco BiTek agar was added (15 g/L) for solid medium. When required for plasmid maintenance, ampicillin was added to minimal and nutrient media at 15 and 150 mg/L, respectively. Unless noted, all chemicals were purchased from Sigma-Aldrich Co. (St. Louis, MO).

Strain	Relevant Genotype
DM3480	<i>ridA3::MudJ</i>
DM9404	Wild type
DM10009	<i>ilvA3210 ridA3::MudJ</i>
DM10010	<i>ridA3::MudJ</i>
DM14171	Wild type/pJF4
DM14172	<i>ridA3::MudJ/pJF4</i>

Table 3.1. Bacterial Strains. MudJ refers to the Mud1734 transposon [20]. The plasmids are derivatives of pBAD24 [21].

3.3.2. Molecular Biology - Construction of JF4.

The pTYB2 (New England Biolabs, IMPACT kit) plasmid was digested with *XbaI* and *NheI* to excise the multiple cloning site and the gene encoding the self-cleaving intein chitin-affinity tag. This fragment was cloned into a pBAD24 [21] plasmid digested with *NheI* and *PstI* to create pJF3. The *glyA* gene was amplified from *S. enterica* LT2 with primers JMF60 (5' CCCCATATGTTAAAGCGTGAAATGAACA TTGC 3') and JMF61 (5' TTACTCGAGTGCGTAAACCGGGAAGCGT 3') using Herculase II Polymerase (Agilent Tech.). Following digestion with *NdeI* and *XhoI*, the gene fragment was cloned into pJF3 digested with *NdeI* and *XhoI* to create pJF4. The final construct was verified by sequencing the ligation junctions.

3.3.3. Ketoacid detection.

Cultures were grown in minimal medium and aliquots were taken periodically. Cells were removed by centrifugation and 3 mL of the cell-free culture medium was incubated at room temperature for 10 minutes with a 1 mL solution of 1% 2,4-dinitrophenylhydrazine (DNPH)

dissolved in 2 N HCl [22, 23]. Next, 4 mL toluene was added and the sample was vortexed at high speed for 30s to selectively extract monocarbonyl-containing α -ketoacids; 3 mL organic (top) layer was moved to a new tube then 3 mL 10% sodium bicarbonate was added and 50 μ L aqueous (bottom) phase was transferred to a microtiter plate containing 150 μ L 1.5 N NaOH and ketoacids were quantified by absorbance at 443 nm in a Lambda Bio 40 spectrophotometer (Perkin Elmer).

3.3.4. HPLC separation of ketoacids and mass spectral analysis.

Ketoacids were extracted as described above. One milliliter of the 10% bicarbonate aqueous phase was spin-dried in a vacufuge (Eppendorf) and resuspended in 200 μ L Solvent A (90:10 10 mM ammonium acetate pH 4.0: acetonitrile). Samples were brought to pH 4.0 with 450 μ L acetic acid and filtered by centrifugation through 0.45 μ m filter (Spin-X). Twenty μ L sample was injected onto an LC-20AT Shimadzu HPLC and separated at room temperature on a Luna 5 μ C18 equilibrated in 30% Solvent B (10:90 10 mM ammonium acetate pH 4.0: acetonitrile), 70% Solvent A. Ketoacid-hydrazones were separated with a gradient at 1 mL/min: 0-10' 70:30 Solvent A:Solvent B, 10-20' gradient to 100% Solvent B, 20-28' 100% Solvent B, 28-30' gradient to 70:30 Solvent A:B. Ketoacid-hydrazones were detected at 340 nm using a Shimadzu SPD-M20A diode array detector and fractions containing relevant ketoacid-hydrazones were submitted for analysis to the mass spectrometry (MS) facility at the University of Wisconsin-Madison Biotechnology Center where they were analyzed by electrospray ionization-mass spectrometry (ESI-MS) in the negative mode. A precursor scan was used to focus on peaks that contained a fragment with a mass of 182, corresponding to the mass of the

cleaved DNPH moiety. Ketoacid hydrazones separated by HPLC were compared to authentic samples subjected to the same derivatization and extraction methods.

3.3.5. Detection of pyruvate in culture supernatants.

To quantify pyruvate, *p*-dimethylbenzaldehyde was used as a derivatizing agent as it does not react with the other ketoacids present [24]. Strains to be tested were grown overnight in 1 ml of rich medium by continuous shaking at 37°C, washed with 100 mM NaCl and inoculated into minimal media with indicated supplements to 12.5% (overnight volume to new culture). Samples were taken periodically and optical density at 650 nm was recorded. The cells were removed by centrifugation (1 minute at 14.8K x g) and the supernatants were frozen at -80°C for further analysis. To determine the pyruvate concentration in the supernatant the following were added to 100 µl of sample: 375 µl of 5 M KOH and 375 µl of *p*-dimethylaminobenzaldehyde solution (4.9 mg/ml methanol). The mixture was allowed to react for 30 minutes at 37 °C after which the absorbance was taken at 420 nm. The concentration of pyruvate in the supernatants was determined using a standard curve generated using defined concentrations of sodium pyruvate. To ensure no interfering compounds were being detected in the assay above, an aliquot of supernatant was depleted of pyruvate using lactate dehydrogenase to reduce pyruvate to lactate using NADH. To deplete pyruvate in 100 µl of supernatant, 5 U of lactate dehydrogenase and 1 µmol NADH were added and allowed to react for 1 hour. Subsequent analysis showed no absorbance corresponding to interfering compounds.

3.3.6. Determination of total coenzyme A in cells.

Total coenzyme A levels were determined using a previously described method [25].

Briefly, strains to be tested were grown overnight in rich medium, washed with 100 mM NaCl and inoculated into minimal media to 2% (overnight culture to new culture). Cultures were grown to an optical density at 650 nm of 0.4, harvested by centrifugation (8000 x g for 12 min.), and frozen at -80 °C for future analysis. Cells were resuspended in phosphate buffered saline and disrupted by the addition of formic acid to 0.25 N and incubation on ice for 30 minutes, vortexing periodically. Cell debris was then separated from lysate by centrifugation (14.8K x g) for 10 minutes. The lysate was then neutralized by the addition of NH₄OH. Aliquots of lysate were treated with 0.7% (w/v) dithiothreitol (DTT) to facilitate reductive cleavage of CoA thioesters. Quantification of CoA was performed by coupled enzymatic assay, the reactions contained the following per mL: 330 µl of DTT-treated lysate, 250 µmol Tris-HCl (pH 7.2), 50 µmol KCl, 15 µmol malate, 6 µmol acetyl-phosphate, 1 µmol NAD⁺, 3.3 U citrate synthase, 15 U malate dehydrogenase and 7.5 U phosphotransacetylase. The rate of NADH formation was monitored at 340 nm. Concentration of CoA was correlated to rate of increase of NADH using authentic standard dilutions.

3.3.7. Serine hydroxymethyltransferase activity.

For crude extract activity determination, strains to be tested were inoculated into rich medium and allowed to grow overnight, spun down and resuspended in NaCl. Minimal medium was inoculated to 2% (overnight culture to new culture), grown to 0.4 OD and harvested by centrifugation (8000 x g for 12 min), and frozen at -80 °C for future analysis. Cell pellets were resuspended in 100 mM potassium phosphate buffer (pH 7.3) with 1 mM ethylenediaminetetraacetic acid (EDTA) and disrupted by sonication. Cell debris was removed by centrifugation (14.8K x g) for 10 minutes. Activity assay was a modification of a previously

described protocol [26] and included the following per mL: 30 μ l clarified cell lysate -or- 1.5 μ g of purified protein, 100 μ mol potassium phosphate (pH 7.2), 0.4 μ mol tetrahydrofolate, 4 nmol pyridoxal 5'-phosphate, 20 μ g FOLD (purified from ASKA collection [27]) and 1 μ mol serine. NADPH evolution was monitored at 340 nm. Glycine production rates were calculated using the extinction coefficient for NADPH at neutral pH ($6.22 \text{ mM}^{-1} \text{ cm}^{-1}$). Protein concentrations were determined using 660 nm Protein Assay (Thermo Scientific) and bovine serum albumin as a reference.

3.3.8. Serine hydroxymethyltransferase purification.

Two liters of minimal medium were inoculated with 50 mL of minimal medium overnight cultures of strains containing JF4 and shaken at 37 °C. When the cultures reached OD_{650} of 0.5, arabinose was added to 0.2% (w/v) final concentration to induce *glyA* expression. Cells were harvested by centrifugation (15 minutes, 9,000 x g) when OD_{650} was between 2-2.5 and the resulting cell pellets were frozen at -80 °C. Pellets were resuspended in 20 mM 4-(2-hydroxyethyl)-1-piperazineethanesulfonic acid (HEPES) , 100 mM sodium chloride buffer (pH 8.5), 5 mM EDTA, 5 mM benzamidine and 10 μ M PLP. Cells were broken with a French Pressure cell (2 passes at 10300 kPa). After clarification by centrifugation (45 min at 48K x g), the supernatant was applied to Chitin resin (column volume 2 mL) and protein purification proceeded per manufacturer's instructions (New England Biolabs, IMPACT). After removal from resin, protein was concentrated and flash frozen in elution buffer with 10% (w/v) glycerol.

3.4. RESULTS AND DISCUSSION

3.4.1. Ketoacids accumulate in growth media of *ridA* mutant strains.

Structural studies performed before the biochemical activity of RidA was defined showed that RidA proteins bind a number of alpha-ketoacids [28, 29]. Partially motivated by these results, the growth media of *ridA* mutants were analyzed for aberrant ketoacid accumulation. Aliquots of supernatant were taken periodically during growth of wild type and *ridA* cultures grown in minimal medium with glucose as the carbon source. In each aliquot, the culture supernatants were treated with dinitrophenylhydrazine to derivatize any monocarboxylic ketoacid and generate stable ketoacid-hydrazones. Total ketoacid-hydrazone concentrations were quantified by measuring absorbance at 443 nm [22, 30]. In both wild type and *ridA* cultures ketoacids accumulated as the cells entered late-log phase and disappeared when cells entered stationary phase (Fig 3.1.A). Significantly, peak accumulation in the *ridA* culture medium was more than 8-fold higher than in the wild-type culture. When succinate or gluconate were utilized as the sole carbon source, ketoacids did not accumulate (data not shown) suggesting glycolytic flux contributed to the effect.

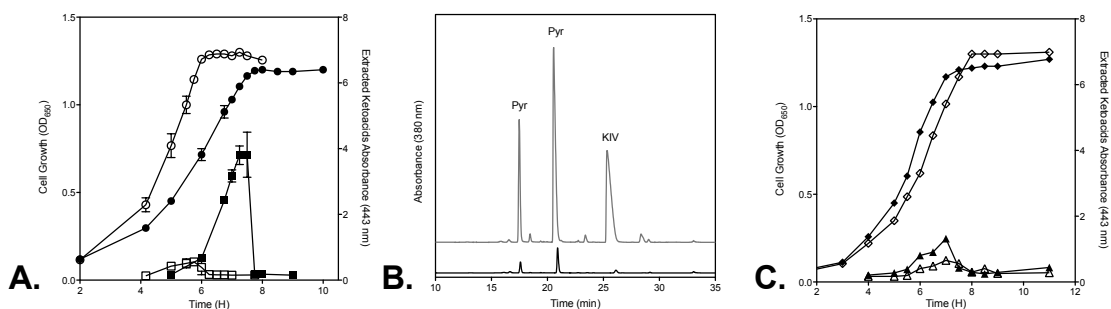


Figure 3.1. Ketoacids accumulate in the culture medium of *ridA* mutants. (A) Wild-type (open symbols) and *ridA* mutant strains (filled symbols) were grown in glucose medium and growth was measured as optical density at 650nm (circles). Monocarbonyl-containing α -ketoacids were detected spectrophotometrically at 443 nm after derivatization and extraction (squares). Data represent two independent cultures. (B) Derivatized α -ketoacids from the culture

medium of WT (black) and a *yjgF* mutant (grey) were separated by HPLC and monitored by absorbance at 380 nm. Ketoacids were identified using derivatized standards of authentic ketoacids and by mass spectral analysis. The hydrazone of pyruvate appeared as two separate peaks at 17 and 20 minutes which were attributed to *syn-anti* isomerization of the pyruvate hydrazone. (C) DM10009 (*ilvA3210 ridA*) was grown in glucose medium (open symbols) while DM10010 (*ridA*) was grown in glucose minimal medium with 0.3 mM isoleucine (closed symbols). Growth of these representative strains was measured as optical density at 650nm (diamonds) and monocarbonyl-containing α -ketoacids were extracted and quantified spectrophotometrically at 443 nm (triangles). Data points were averaged from two independent cultures.

Hydrazones in the dinitrophenylhydrazine-derivatized supernatants were separated by HPLC and monitored at 443 nm (Figure 3.1.B). The identities of the precursor ketoacids were determined by using authentic standards and mass spectrometry analyses. Pyruvate was the major ketoacid in both supernatants and in the *ridA*-culture-supernatant ketoisovalerate (KIV) was also detected. These data showed that the absence of RidA resulted in a significant imbalance in the metabolic network resulting in pyruvate accumulation.

3.4.2. Mutants lacking RidA accumulate pyruvate due to lowered CoA levels.

The increased level of KIV was not completely unexpected given that the activity of transaminase B (IlvE) is reduced in a *ridA* strain [14, 16]. IlvE is responsible for the generation of isoleucine and valine from ketomethylvalerate and ketoisovalerate, respectively (Figure. 3.2). Pyruvate accumulation was pursued because it was not an expected consequence of decreased

transaminase B activity, making it likely that this phenotype was a consequence of *ridA* mutation that had not previously been identified. Pyruvate is utilized by three main enzymes; pyruvate dehydrogenase (PDH), pyruvate formate lyase (PFL) and pyruvate oxidase (POX), none of which are PLP-dependent. When assayed in crude extract, no difference in activity can be detected of these enzymes between *ridA* and wild-type strains (data not shown).

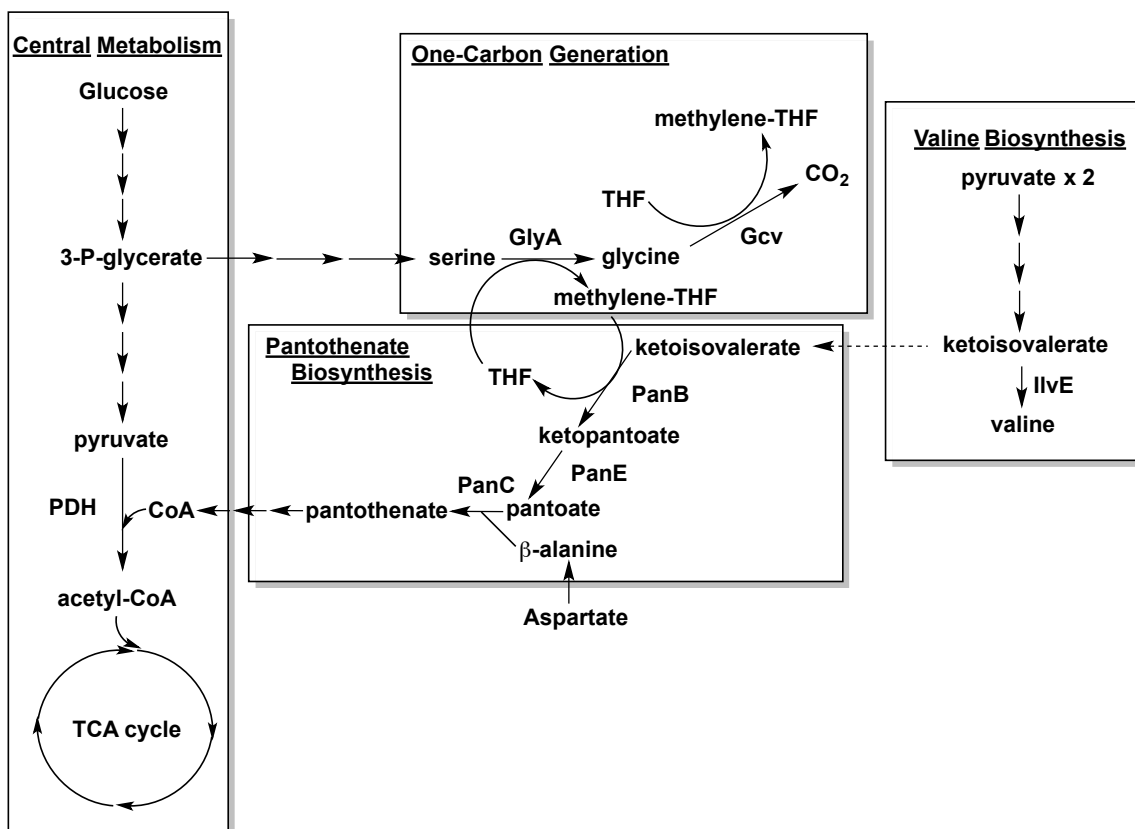


Figure 3.2. The metabolic interconnection of glycolysis, one-carbon metabolism, valine biosynthesis and pantothenate biosynthesis. Shown are the metabolic pathways and connections contributing to the generation of coenzyme A in *S. enterica*, where: PDH = pyruvate dehydrogenase; Gcv = glycine cleavage complex; GlyA = serine hydroxymethyltransferase; PanB = ketoisovalerate hydroxymethyltransferase; PanE = ketopantoate reductase; PanC = pantothenate synthetase; IlvE = transaminase C.

PDH, responsible for the bulk of aerobic pyruvate catabolism, uses coenzyme A (CoA) as a co-substrate. Radmacher *et al.* showed that mutations in the pantothenate biosynthetic genes *panBC* of *C. glutamicum* decreased the intracellular concentration of CoA and resulted in the accumulation of pyruvate [31]. Based on this precedent, pantothenate was added to the medium to raise internal CoA levels and then pyruvate accumulation was measured in a *ridA* strain. Exogenous pantothenate eliminated the bulk of pyruvate accumulation by a *ridA* strain (Figure 3.3A), suggesting that the pyruvate accumulation was the result of decreased CoA pools.

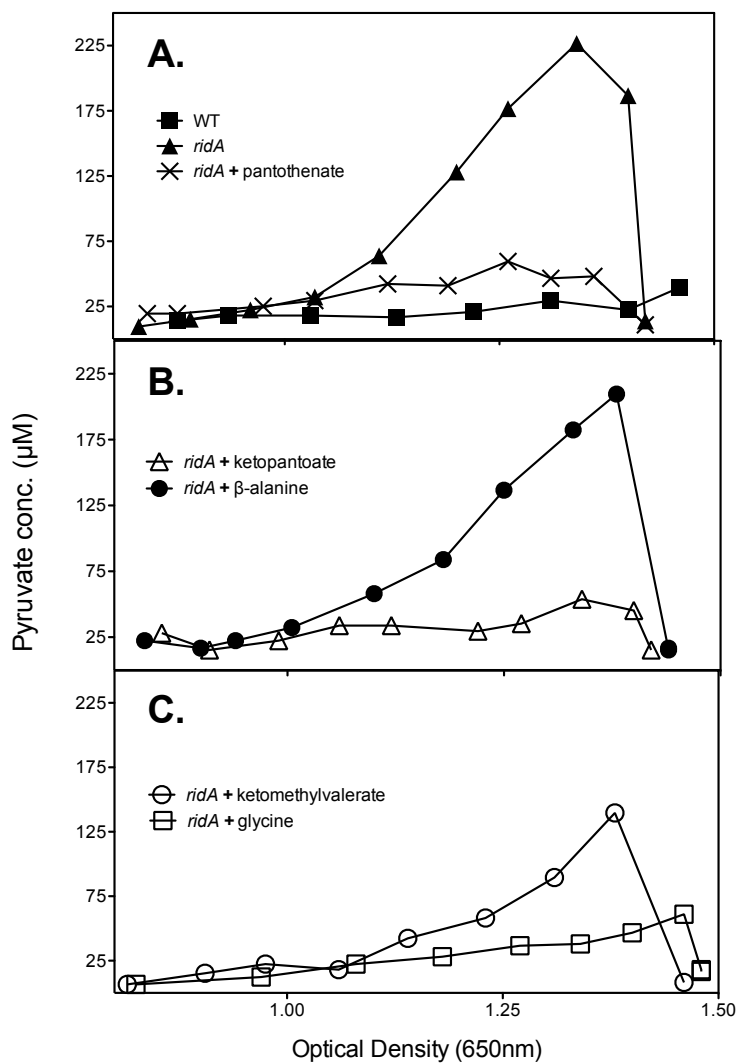


Figure 3.3. *ridA* mutants excrete pyruvate. The data are representative curves showing pyruvate concentrations throughout growth of wild type (DM9404) and *ridA* mutant (DM3480) with indicated supplements. Data are represented as pyruvate concentration vs. optical density in order to compare cultures with differing growth rates at the same growth phase.

Consistent with this interpretation, total CoA levels were 2.8-fold less in a *ridA* strain than those found in the wild type. Furthermore, exogenous pantothenate restored the CoA levels in a *ridA* strain (Table 3.2).

Strain	Genotype	Supplement	Total CoA (nmol CoA mg ⁻¹ dry weight)	% Wild type
DM9404	Wild type	-	2.02 ± 0.06	
DM3480	<i>ridA</i>	-	0.68 ± 0.06	34
DM3480	<i>ridA</i>	pantothenate	2.12 ± 0.18	105
DM3480	<i>ridA</i>	glycine	1.68 ± 0.13	83
DM3480	<i>ridA</i>	isoleucine	1.78 ± 0.16	88

Table 3.2. Total CoA levels are lowered in *ridA* strain. Total CoA was measured in cell pellets of the indicated strains grown in the presence and absence of supplements. Data given are the mean and standard deviation of experiments performed in biological duplicate with technical triplicates.

3.4.3. Lowered CoA levels in *ridA* mutants are due to a defect in one-carbon metabolism.

The data above suggested that despite the lack of a PLP-dependent enzyme in this pathway, pantothenate biosynthesis was compromised in a *ridA* strain. The compromised branch of pantothenate biosynthesis (Figure 3.2) was determined by adding exogenous 2-ketopantoate or β -alanine to the medium and monitoring pyruvate accumulation during growth (Figure 3.3.B). Exogenous 2-ketopantoate abolished pyruvate accumulation, while the addition of β -alanine had no effect. 2-ketopantoate is derived from KIV and data discussed above showed that KIV accumulated in the growth medium of *ridA* mutants. Taken together these results suggested that the enzymatic step catalyzed by ketoisovalerate hydroxymethyltransferase (PanB) was compromised in a *ridA* strain. This conclusion was consistent with the finding that exogenous addition of KIV (100 μ M) lowered but did not eliminate pyruvate accumulation (Figure 3.3.C).

The enzymatic step catalyzed by PanB utilizes the cosubstrate 5,10-methylene-tetrahydrofolate to formylate KIV to generate 2-ketopantoate (Figure 3.2). Thus, a limitation for the 1-carbon unit carrier 5,10-methylene-tetrahydrofolate could explain the lowered CoA levels detected in a *ridA* strain. To bolster 5,10-methylene-tetrahydrofolate levels exogenous glycine was added to *ridA* culture as degradation of glycine by the inducible glycine cleavage complex generates 5,10-methylene-tetrahydrofolate [32]. The addition of glycine to the growth medium reduced the pyruvate accumulation in the culture of a *ridA* strain (Fig 3.3.C). This result led to the hypothesis that *ridA* strains are limited for 5,10-methylene tetrahydrofolate (Fig. 3.2). The exogenous addition of glycine also significantly increased the CoA levels in a *ridA* strain (Table 3.2). Taken together, these results suggested that under these growth conditions *ridA* mutants lacked sufficient 5,10-methylene tetrahydrofolate to generate 2-ketopantoate to satisfy the

demand for coenzyme A. Further, these data suggested that a defect in one-carbon unit synthesis was responsible for the lowered CoA levels in a *ridA* mutant.

3.4.4. *ridA* mutants have lowered serine hydroxymethyltransferase activity.

During growth on glucose, *S. enterica* derives one-carbon units from the conversion of serine to glycine *via* the PLP-containing enzyme serine hydroxymethyltransferase (GlyA) [33]. When assayed in cell-free extracts, GlyA activity was more than 5-fold decreased in *ridA* strains compared to wild type strains (Table 3.3). The activity of GlyA was not affected by the addition of pantothenate to the medium, indicating that while pantothenate increased CoA levels, it did so by acting downstream of the GlyA catalyzed reaction.

Strain	Genotype	Supplement	Activity (nmol glycine min ⁻¹ mg ⁻¹)	Percent of wild type
DM9404	Wild type	-	27.9 ± 4.9	
DM3480	<i>ridA</i>	-	4.8 ± 1.8	17
		pantothenate	5.7 ± 2.7	20
		isoleucine	11.3 ± 1.2	40

Table 3.3. Serine hydroxymethyltransferase activity in crude extract. Serine hydroxymethyltransferase activity was assayed in sonicated cell lysate of the indicated cells. Cultures were grown in the presence or absence of indicated supplements. Data given are mean and standard deviation of biological triplicate with technical duplicate.

3.4.5. GlyA isolated from a *ridA* strain had reduced specific activity and distinct spectral characteristics.

To determine the nature of GlyA inhibition, the enzyme was overproduced and purified to >95% purity from wild type and *ridA* backgrounds in the presence of PLP cofactor. The hydroxymethyltransferase specific activity of the protein isolated from the *ridA* background was 25% lower than the protein isolated from the wild type strain (1.47 ± 0.08 and 1.14 ± 0.05 $\mu\text{mol glycine min}^{-1} \text{mg}^{-1}$ for wild type and *ridA* isolated protein, respectively). The decreased specific activity indicated that the inhibited GlyA was stable through purification, consistent with a causative post-translational modification.

The enzyme preparations from a wild-type strain and from a *ridA* strain had different spectral properties. As shown in Figure 3.4.A, enzymes isolated from both strain backgrounds had the absorbance at 420 nm that is characteristic of a PLP internal aldimine. Similar absorbance between the two samples indicated roughly the same amount of cofactor was bound to the protein in each preparation. The addition of substrates glycine and tetrahydrofolate shifted the absorbance spectra of GlyA, decreasing the absorbance at 420 nm and generating a peak absorbing at 490 nm that corresponds to a quinoid species generated when glycine loses an α -proton and forms a carbanion in resonance with the PLP ring [34] (Figure 3.5.A). As expected, after addition of glycine and tetrahydrofolate to the GlyA preparation isolated from wild-type, the peak at 420 nm is decreased with the simultaneous appearance of a peak at 490 nm indicating formation of the quinoid intermediate (Figure 3.4.B). However, after the addition of substrates to the enzyme isolated from the *ridA* strain, only a partial spectral shift was observed, suggesting the formation of the quinoid species was blocked (Figure 3.4.B). A rough quantitation by integrating the area under the curve of the 490 nm peak (normalized to the minimum at 470 nm), found the protein isolated from *ridA* had 73% of the absorbance as the protein purified from the wild type (8.80 and 6.46, wildtype and *ridA* background respectively). This ratio correlated with

the respective activities of the two enzyme preparations. From these data we concluded that the GlyA protein isolated from a *ridA* strain had a post-translational modification that did not affect cofactor binding but prevented binding of the substrates and/or the abstraction of the α -proton of the bound glycine.

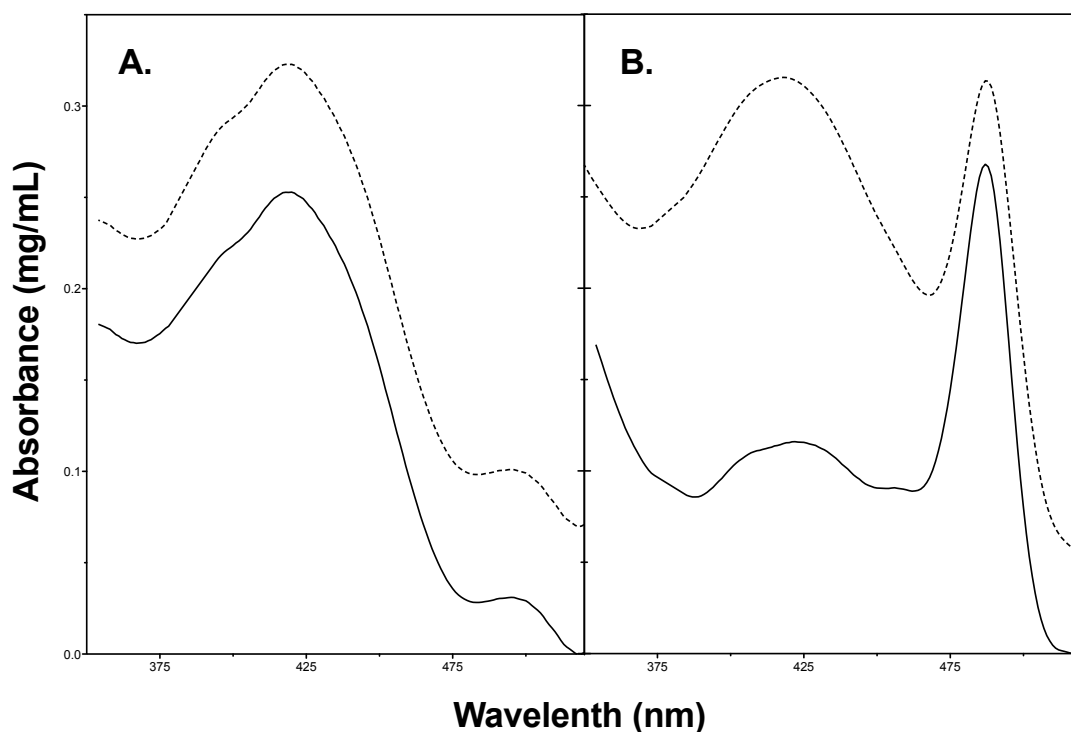


Figure 3.4. Spectral characteristics of *ridA*-isolated GlyA differ from wild type-isolated GlyA. Protein isolated from wild type and *ridA* mutant strains were assessed for differing visible spectral characteristics. (A) Spectra of GlyA isolated from wildtype (-) and *ridA* mutant (--) in 100 mM potassium phosphate at pH 7.2 are comparable. (B) Spectra after the addition of glycine (20 mM) and tetrahydrofolate (0.18 mM).

The inhibition of PLP-containing enzymes by 2-AA has been characterized to proceed through two routes: (1) 2-AA attacks the internal aldimine of the cofactor (*i.e.* alanine racemase) [8, 9] and (2) 2-AA first forms an external aldimine which is attacked by a nucleophilic residue

in the active site to generate a thioester or ester from cysteine or glutamate/aspartate, respectively (*i.e.*, IlvE, aspartate decarboxylase) shown in Figure 3.5.B [13].

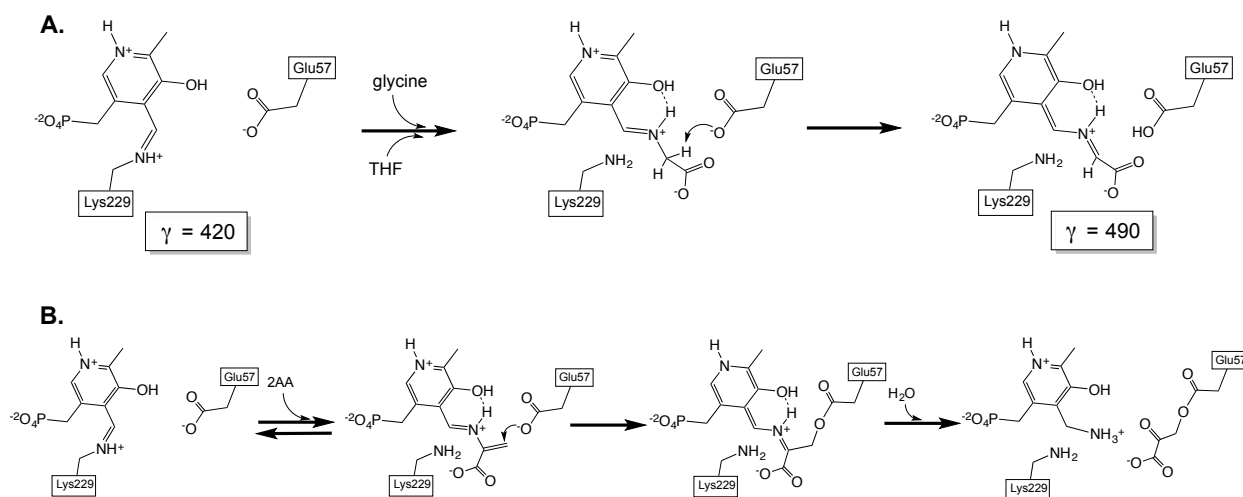


Figure 3.5. GlyA active site configuration and proposed modification scheme. (A) Native serine hydroxymethyltransferase with internal aldimine to the PLP cofactor absorbs at 420 nm, after the addition of glycine and tetrahydrofolate glycine and PLP form an external aldimine and the subsequent extraction of an α -proton of glycine generates a species that absorbs at 490 nm. (B) Inactivation scheme similar to that proposed previously for aspartate decarboxylase [(Relyea, 1974)] whereby 2-aminoacrylate forms external aldimine with active site cofactor and then is attacked by nucleophilic glutamate residue, the cofactor can then be released as pyridoxamine phosphate and glutamate is esterified to the pyruvoyl moiety after hydrolysis.

Treatment of mammalian GlyA with the 2-AA-generating molecule D-fluoroalanine implicated the second route above with an active site cysteine residue becoming covalently modified [35]. However the crystal structure of GlyA from *E. coli* (PDB 1DFO, [36]) reveals that the closest cysteine residue lies >12 Å away from the active site. The only nucleophilic

residue in the proximity of the active site in GlyA from *S. enterica* is the highly conserved glutamate 57. Based on this active site structure, we suggest GlyA is being inactivated by the scheme in Figure 3.5B. This mechanism is similar to aspartate decarboxylase [13], where 2-AA forms an external aldimine in the active site and then is attacked by the nucleophilic Glu57, subsequent rearrangements and hydrolysis result in an esterified glutamate residue and the release of pyridoxamine phosphate. The resulting modification described above is unstable due to the ester bond, which is readily hydrolysable. Consistent with this, after the GlyA protein isolated from *ridA* mutant strain was dialyzed overnight in 30 mM phosphate buffer (pH 7.2), the specific activity was increased and the spectral features became similar to the protein purified from a wild-type strain (DNS). These results are consistent with an unstable modification and could explain the difficulty in obtaining an accurate mass for the modified protein.

3.4.6. Threonine dehydratase activity is responsible for decreasing GlyA activity.

Previous studies showed the activity of the biosynthetic enzyme, threonine dehydratase (IlvA), was responsible for several *ridA* mutant phenotypes [15, 16, 18]. Recent research showed that 2-aminoacrylate generated from serine by IlvA inhibited IlvE *in vitro* [14]. The activity of IlvA, and thus its deleterious effects in a *ridA* mutant, are prevented by the allosteric inhibitor, isoleucine. Addition of isoleucine to the growth medium of a *ridA* strain, or presence of an IlvA variant with a lowered specific activity [15] prevented ketoacid accumulation (Figure 3.1.C). Also, growth of a *ridA* mutant with exogenous isoleucine increased CoA levels to 80% of those found in a wild type strain (Table 3.2) and doubled the activity of GlyA to 40% that of wild type (Table 3.3). Taken together these results suggested the serine deaminase activity of IlvA is involved, but not the only source of 2-AA that inhibits GlyA in the absence of RidA.

3.5. CONCLUSIONS

This study was initiated to explain a *ridA* mutant phenotype in the context of the biochemical activity recently attributed to the protein family. *S. enterica* strains lacking RidA aberrantly accumulated pyruvate in the growth medium. A combination of *in vivo* and *in vitro* approaches found PLP-dependent serine hydroxymethyltransferase was at the root of this phenotype. The data showed that decreased activity of GlyA led to decreased 5,10-methylene tetrahydrofolate availability that resulted in constrained flux at the PanB enzymatic step. The resulting decrease in pantothenate synthesis lowered the total CoA pool. Ultimately the CoA limitation generated a constraint in the glycolytic breakdown of pyruvate leading to pyruvate accumulation in the growth media.

The finding that serine hydroxymethyltransferase activity was 5-fold lower in a *ridA* mutant emphasized the importance of the RidA protein family for maintaining a robust metabolism. In the growth conditions tested, approximately 10% of the total carbon from glucose would flow through this enzyme. An estimated 5% of the carbon in glucose is required to meet the one-carbon demands of *E. coli* when growing in minimal media to synthesize purines, histidine, methionine, pantothenate and to methylate DNA and RNA (while another 5% is required to meet the demands for glycine) [33]. Based on the central role of GlyA, it was somewhat surprising that the notable phenotype of decreased activity was in a distant branch of the metabolic network.

This work increased our knowledge of the PLP enzymes that are inactivated by 2-AA when RidA is absent and demonstrated the complexity of identifying defects in the metabolic network. Furthermore, it highlighted the importance of thorough characterization of *ridA* mutant

strains to determine the effect of 2-AA on cellular physiology. Thus far threonine dehydratase (IlvA) is the only cellular enzyme demonstrated to be significant in generating 2-AA *in vivo*. The data herein suggest that this enzyme also contributes to the inactivation of GlyA. However, the inability of the allosteric effector isoleucine to completely restore GlyA activity provides evidence that additional enzymes are contributing to the metabolic stress caused by enamines. This result implicates additional cellular sources of 2-AA and necessitates further inquiry to elucidate the full extent of 2-AA producers in the cell. This work contributed to our understanding of the physiological effects of removing RidA and indicated that additional studies in *S. enterica* and other organisms will be required to dissect the breadth of the metabolite stress system that was uncovered with the characterization of this protein family.

3.6 REFERENCES

1. Leitner-Dagan, Y., et al., *CHRD, a plant member of the evolutionarily conserved YjgF family, influences photosynthesis and chromoplastogenesis*. *Planta*, 2006. 225(1): p. 89-102.
2. Lambrecht, J.A., J.M. Flynn, and D.M. Downs, *Conserved YjgF protein family deaminates reactive enamine/imine intermediates of pyridoxal 5'-phosphate (PLP)-dependent enzyme reactions*. *J Biol Chem*, 2012. 287(5): p. 3454-61.
3. Oxelmark, E., et al., *Mmf1p, a novel yeast mitochondrial protein conserved throughout evolution and involved in maintenance of the mitochondrial genome*. *Mol Cell Biol*, 2000. 20(20): p. 7784-97.

4. Eliot, A.C. and J.F. Kirsch, *Pyridoxal phosphate enzymes: mechanistic, structural, and evolutionary considerations*. *Annu Rev Biochem*, 2004. 73: p. 383-415.
5. Hillebrand, G.G., J.L. Dye, and C.H. Suelter, *Formation of an intermediate and its rate of conversion to pyruvate during the tryptophanase-catalyzed degradation of S-o-nitrophenyl-L-cysteine*. *Biochemistry*, 1979. 18(9): p. 1751-5.
6. Schnackerz, K.D., et al., *Mechanism of action of D-serine dehydratase. Identification of a transient intermediate*. *Biochemistry*, 1979. 18(16): p. 3557-63.
7. Zhao, Z. and H. Liu, *A quantum mechanical/molecular mechanical study on the catalysis of the pyridoxal 5'-phosphate-dependent enzyme L-serine dehydratase*. *J Phys Chem B*, 2008. 112(41): p. 13091-100.
8. Badet, B., D. Roise, and C.T. Walsh, *Inactivation of the dadB Salmonella typhimurium alanine racemase by D and L isomers of beta-substituted alanines: kinetics, stoichiometry, active site peptide sequencing, and reaction mechanism*. *Biochemistry*, 1984. 23(22): p. 5188-94.
9. Esaki, N. and C.T. Walsh, *Biosynthetic alanine racemase of Salmonella typhimurium: purification and characterization of the enzyme encoded by the alr gene*. *Biochemistry*, 1986. 25(11): p. 3261-7.
10. Kishore, G.M., *Mechanism-based inactivation of bacterial kynureninase by beta-substituted amino acids*. *J Biol Chem*, 1984. 259(17): p. 10669-74.
11. Likos, J.J., et al., *A novel reaction of the coenzyme of glutamate decarboxylase with L-serine O-sulfate*. *Biochemistry*, 1982. 21(18): p. 4377-86.

12. Relyea, N.M., S.S. Tate, and A. Meister, *Affinity labeling of the active center of L-aspartate-beta-decarboxylase with beta-chloro-L-alanine*. J Biol Chem, 1974. 249(5): p. 1519-24.
13. Tate, S.S., N.M. Relyea, and A. Meister, *Interaction of L-aspartate beta-decarboxylase with beta-chloro-L-alanine. Beta-elimination reaction and active-site labeling*. Biochemistry, 1969. 8(12): p. 5016-21.
14. Lambrecht, J.A., G.E. Schmitz, and D.M. Downs, *RidA proteins prevent metabolic damage inflicted by PLP-dependent dehydratases in all domains of life*. MBio, 2013. 4(1): p. e00033-13.
15. Christopherson, M.R., G.E. Schmitz, and D.M. Downs, *YjgF is required for isoleucine biosynthesis when Salmonella enterica is grown on pyruvate medium*. J Bacteriol, 2008. 190(8): p. 3057-62.
16. Schmitz, G. and D.M. Downs, *Reduced transaminase B (IlvE) activity caused by the lack of yjgF is dependent on the status of threonine deaminase (IlvA) in Salmonella enterica serovar Typhimurium*. J Bacteriol, 2004. 186(3): p. 803-10.
17. Browne, B.A., A.I. Ramos, and D.M. Downs, *PurF-independent phosphoribosyl amine formation in yjgF mutants of Salmonella enterica utilizes the tryptophan biosynthetic enzyme complex anthranilate synthase-phosphoribosyltransferase*. J Bacteriol, 2006. 188(19): p. 6786-92.
18. Enos-Berlage, J.L., M.J. Langendorf, and D.M. Downs, *Complex metabolic phenotypes caused by a mutation in yjgF, encoding a member of the highly conserved YER057c/YjgF family of proteins*. J Bacteriol, 1998. 180(24): p. 6519-28.

19. Davis, R.W., D. Botstein, and J. R. Roth, *Advanced bacterial genetics*. 1980, Cold Spring Harbor, N.Y.: Cold Spring Harbor Laboratory.
20. Castilho, B.A., P. Olfson, and M.J. Casadaban, *Plasmid insertion mutagenesis and lac gene fusion with mini-mu bacteriophage transposons*. *J Bacteriol*, 1984. 158(2): p. 488-95.
21. Guzman, L.M., et al., *Tight regulation, modulation, and high-level expression by vectors containing the arabinose PBAD promoter*. *J Bacteriol*, 1995. 177(14): p. 4121-30.
22. Friedemann, T.E.H., G. E., *The determination of ketoacids in blood and urine*. *J Biol Chem*, 1943. 147: p. 415-441.
23. Raunio, R., *Accumulation of keto acids during the growth cycle of Escherichia coli*. *Acta Chem Scand*, 1966. 20(1): p. 11-6.
24. Holtzclaw, W.D. and L.F. Chapman, *A new assay for transaminase C*. *Anal Biochem*, 1977. 83(1): p. 162-7.
25. Allred, J.B. and D.G. Guy, *Determination of coenzyme A and acetyl CoA in tissue extracts*. *Anal Biochem*, 1969. 29(2): p. 293-9.
26. Schirch, V.M., M, *Serine Transhydroxymethylase: Spectral Properties of the Enzyme-bound Pyridoxal-5-phosphate*. *J Biol Chem*, 1962. 237: p. 2578-2581.
27. Kitagawa, M., et al., *Complete set of ORF clones of Escherichia coli ASKA library (a complete set of E. coli K-12 ORF archive): unique resources for biological research*. *DNA Res*, 2005. 12(5): p. 291-9.
28. Burman, J.D., et al., *The crystal structure of Escherichia coli TdcF, a member of the highly conserved YjgF/YER057c/UK114 family*. *BMC Struct Biol*, 2007. 7: p. 30.

29. Parsons, L., et al., *Solution structure and functional ligand screening of HI0719, a highly conserved protein from bacteria to humans in the YjgF/YER057c/UK114 family.* Biochemistry, 2003. 42(1): p. 80-9.
30. Dawson, R.M.E., D.; Elliott, W., Jones, K. M., *Data for Biochemical Research*1986, Oxford: Clarendon Press.
31. Radmacher, E., et al., *Linking central metabolism with increased pathway flux: L-valine accumulation by Corynebacterium glutamicum.* Appl Environ Microbiol, 2002. 68(5): p. 2246-50.
32. Stauffer, G.V., L.T. Stauffer, and M.D. Plamann, *The Salmonella typhimurium glycine cleavage enzyme system.* Mol Gen Genet, 1989. 220(1): p. 154-6.
33. Matthews, R.G., *One-carbon metabolism, in Escherichia coli and Salmonella typhimurium Cellular and Molecular Biology*, F.C. Neidhardt, Editor 1996, American Society for Microbiology: Washington. p. 506-513.
34. Schirch, V., et al., *Serine hydroxymethyltransferase from Escherichia coli: purification and properties.* J Bacteriol, 1985. 163(1): p. 1-7.
35. Wang, E.A., R. Kallen, and C. Walsh, *Mechanism-based inactivation of serine transhydroxymethylases by D-fluoroalanine and related amino acids.* J Biol Chem, 1981. 256(13): p. 6917-26.
36. Scarsdale, J.N., et al., *Crystal structure at 2.4 Å resolution of E. coli serine hydroxymethyltransferase in complex with glycine substrate and 5-formyl tetrahydrofolate.* J Mol Biol, 2000. 296(1): p. 155-68.

CHAPTER 4

Summary, Conclusions, Future Directions, and Final Comments

4.1. SUMMARY AND CONCLUSIONS

4.1.1 Overview

The goal of this research was to further define the cellular role of the RidA protein family. This work built on established research of the physiological characteristics of *ridA* mutants [1-3] and the enamine deaminase activity of RidA [4]. The data here give direct evidence of 2-aminoacrylate accumulation in strains lacking RidA and expand our understanding of *ridA* physiology by adding three enzymes which are inhibited in *ridA* strains and by characterizing the one-carbon metabolic defect in *ridA* mutants.

4.1.2 *ridA* mutants contain 2-aminoacrylate-modified Alr enzymes

ridA mutants are compromised in their ability to utilize L-alanine as their sole nitrogen source. However, these mutants are able to utilize D-alanine as a sole nitrogen source. This growth phenotype suggested a compromised alanine racemase activity in *ridA* strains. Crude extract assays confirmed the alanine racemase activity was forty percent lower in *ridA* strains relative to wild type. Mutant analysis confirmed a *ridA* mutant dependent defect in the catabolic alanine racemase, DadX, but further steps were taken to overexpress the biosynthetic racemase, Alr, and show that it was compromised as well.

Purification of the biosynthetic racemase showed the enzyme had a stable inhibitory modification. To determine nature of this modification, the protein was denatured and was

analyzed for cofactor content; a decrease in PLP cofactor was found for protein isolated from *ridA* strain. Furthermore, cofactor analysis of Alr with HPLC showed an additional cofactor species in Alr isolated from *ridA* mutants. Mass spectral analysis confirmed that the species was aminoacrylate modified-PLP. These results show that alanine racemase is exposed to, and inhibited by, 2-AA in *ridA* mutant strains *in vivo*. Evidence of 2-AA inhibition of Alr gives authority to the proposed *in vivo* role of RidA to mitigate toxicity via 2-AA.

4.1.3 *ridA* mutants accumulate pyruvate due to compromised serine hydroxymethyltransferase activity

ridA mutants were found to excrete pyruvate during exponential phase of growth on glucose. In an attempt to further define *ridA* mutant physiology, the root cause of this phenotype was investigated. Pyruvate excretion was shown to be the result of a bottleneck at the conversion of pyruvate to acetyl-CoA via pyruvate dehydrogenase due to coenzyme A being limiting. Metabolite feeding traced the excretion of pyruvate to a defect in one-carbon metabolism whereby the addition of glycine would correct both the defect in CoA levels and the excretion of pyruvate.

Under the tested growth conditions, *S. enterica* derives its one-carbon units from the conversion of serine to glycine via the serine hydroxymethyltransferase, GlyA [5]. Subsequent activity assays of lysed cells revealed a significant defect in GlyA activity. The activity defect was unaffected by glycine or pantothenate addition showing that though the phenotype is corrected, the enzyme is still susceptible to inactivation. GlyA purified from *ridA* strains showed a defect in activity and differing spectral characteristics when compared to protein isolated from a wild type strain. These results suggested GlyA was post-translationally modified. The

susceptibility of GlyA to 2-AA generated via serine *o*-sulfate *in vitro* has been previously reported [6]. Combining this susceptibility with the reported accumulation of 2-AA in *ridA* strains reported here and elsewhere [7], we hypothesize that 2-AA inhibition is the cause of the GlyA activity defect. Attempts were made to characterize inhibited GlyA with mass spectrometry; however, they were unsuccessful perhaps due to the unstable nature of the modification. These results further characterize the differences in *ridA* mutant physiology due to the inhibiting effect of 2-AA, showing disparate areas of metabolism are effected by the deletion of *ridA*.

4.2 FUTURE DIRECTIONS

4.2.1 Serine Metabolism and leucine responsive protein

The results above implicated the activity of threonine dehydratases, IlvA, in the generation of 2-AA *in vivo*. Two key factors likely influence the need for RidA requirement at this step: (1) isoleucine is only generated by 2-ketobutyrate generated by PLP-dependent threonine dehydratase, and (2) serine is kept at a sufficiently high level such that IlvA generates 2-AA at a basal rate whenever active. It is striking that another route to produce isoleucine has not evolved given the stress 2-AA can have on the cell. Perhaps given the effectiveness and ubiquity of RidA, there exists little to no selective pressure to obtain isoleucine via a different route. Additionally, it seems that serine cannot be simply kept at a concentration low enough so that it not acted upon by IlvA despite the deleterious generation of 2-AA or the waste of energy incurred. We can suppose that the use of serine as a precursor to a number of cellular metabolites and its requirement for protein synthesis affect the basal level of serine required for efficient metabolism. So, it seems that evolution has favored a cellular concentration of serine that still

results in 2-AA generation, presumably in order to enable the reactions for which serine is required.

Given the danger posed by serine breakdown via PLP-dependent mechanisms, the manner in which the cell deals with excess serine will give further insights into how the cell mitigates 2-AA stress. The canonically characterized route of serine degradation is via iron sulfur cluster-containing enzymes that share structural identity to aconitase [8]. Given their similarity to aconitase, it has been suggested that these enzymes will not release 2-AA but rather dehydrate and rehydrate/deaminate before releasing the substrate, thus circumventing the production of 2-AA. Furthermore, *in vitro* assays that probed IlvE inactivation in the presence of serine and SdaA showed no evidence for inactivation (Grischa Chen, *unpublished*). Subsequently it appears that the way the cell controls serine concentration circumvents the production of 2-AA. In fact, there is a large amount of redundancy in the expression of Fe-S serine deaminases in *E. coli*, where three homologs, (SdaA, SdaB, and TdcG) are expressed differentially under all conditions [9].

Future efforts would be well served to further understand the metabolic network surrounding serine biosynthesis and catabolism. It would seem that serine concentrations would need to be tightly regulated to ensure it is of sufficient levels to be used in biosynthetic reactions but not in great excess as any accumulation may result in the generation of 2-AA. The serine metabolic connections are summed in Figure 4.1.

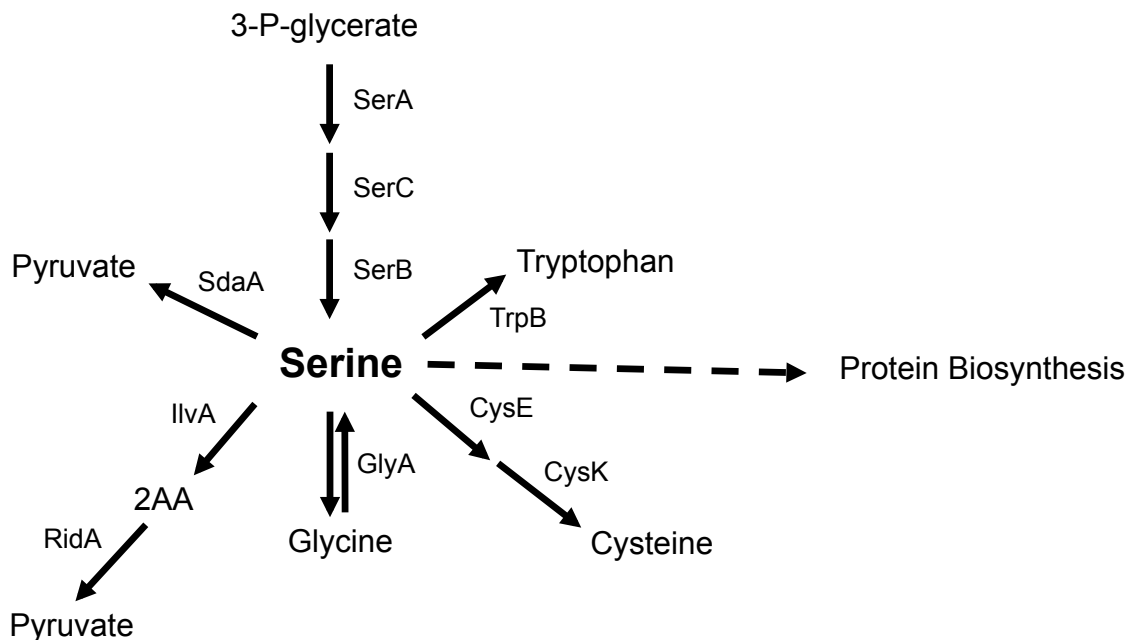


Figure 4.1. Serine metabolic node. Serine is generated from 3-phosphoglycerate via SerACB (3-phosphoglycerate dehydrogenase, 3-phosphoserine aminotransferase, phosphoserine phosphatase, respectively) and from glycine via GlyA (serine hydroxymethyltransferase). Serine can be broken down into pyruvate via SdaA (serine deaminase) and to 2AA (2-aminoacrylate) via IlvA (threonine dehydratase). Serine is used biosynthetically for protein biosynthesis and amino acid biosynthesis. Cysteine is generated from serine via CysE (serine acetyltransferase) and CysK (cysteine synthase). The final step in tryptophan biosynthesis is catalyzed by TrpB (tryptophan synthase) which condenses indole and dehydrated serine. *Information obtained from Ecocyc.org database <www.ecocyc.org>.*

When one looks at the regulation of all of the pathways connected to the serine metabolic node, there is the recurring thread of regulation via leucine responsive protein, Lrp. The Lrp regulon is not fully defined yet it is predicted to regulate at least 10% of genes in *E. coli* [10]. Despite extensive study [11] the precise function and regulatory scheme are not fully

understood. Contained within the regulon are operons that are induced, repressed and non-responsive to leucine addition. Interestingly, Lrp has preliminary links to RidA. In *E. coli*, there exists a sequence 17 base pairs upstream of the *ridA* start codon (AGACTTTTACCG) that is similar to the published consensus binding sequence of Lrp (AGAATTTTATTCT). In Chapter 3, accumulation of the leucine precursor ketoisovalerate was shown. Though it has not been investigated, I hypothesize that that leucine accumulation results from 2-AA stress and this accumulation of leucine causes Lrp-mediated upregulation of serine catabolic genes (*i.e.* SdaA) and RidA while simultaneously downregulating serine biosynthesis genes (SerACB).

4.2.2 Identification of new targets of 2-aminoacrylate inhibition

Detailed in Chapter 2 and Chapter 3 are two essential enzymes that become modified by 2-AA in *ridA* strains and modification of IlvE has been described previously [7]. These enzymes generate a theme of PLP-containing enzyme inhibition and the proposed inhibition schemes rely on the PLP cofactor for modification. A more directed look at PLP enzyme activity in *ridA* mutants would certainly yield more targets of inhibition. The identification of the full range of enzymes inhibited will help to generate a panorama of 2-AA inhibition in the cell.

One approach that may prove useful for predicting other targets of 2AA *in vivo* is the survey of the structures of PLP-containing enzymes. Given the two routes of inhibition discussed throughout this body of work structures can be evaluated for (1) the presence of nucleophilic groups near the active site lysine and (2) the space around the PLP-lysine aldimine which may allow for attack by 2-AA. This technique will have its pitfalls given that the static portrait of crystal structures do not reveal the range of conformations proteins assume in solution. For instance, a study of the crystal structure of IlvE suggested that a glutamic acid residue near the

active site may be susceptible to modification due to its proximity to the active site. However, site directed mutagenesis of this glutamate to an alanine resulted in a protein that was still modified and inactivated [7]. From the crystal structure, no other putative residues were apparent given the proposed mechanism. Given this test case, elucidation of inhibition from structure is not trivial but may help with hypothesis development.

Further genetic approaches may also be helpful in the elucidation of new targets. In Appendix B, I detail the construction of a strain designed to overproduce 2-AA through the inducible overexpression of the degradative threonine dehydratase, TdcB. This strain will exacerbate 2-AA inhibition phenotypes, making their effect more profound. Fortuitously, this effect of *tdcB* overexpression revealed a new phenotype in the proof-of-concept experiment. The expression of *tdcB* in a *ridA* strain exacerbated a PLP-biosynthesis defect that previous experiments in *ridA* mutant strains had hinted was occurring. New rounds of screening with *ridA* mutants overexpressing *tdcB* will reveal new phenotypes that were too subtle to be identified in strains only lacking RidA.

4.3 FINAL COMMENTS

A tremendous amount of effort has been put into determining the role of the RidA family of proteins. Genetic, structural, biochemical, and physiological approaches were needed to tease out RidA activity and role due to the nuanced effects that result from its removal from cells. This research was performed at a fortunate crossroads: the biochemical activity of RidA was newly defined and there was a wealth of physiological observations available. This work helped to establish and solidify 2-aminoacrylate as a *bona fide* cellular stressor and further characterize its deleterious effects on cellular metabolism.

Given the observations that 2-AA can covalently inhibit certain PLP-containing enzymes *in vitro* and 2-AA is generated from a number of reactions, it is surprising that no one ever hypothesized the concurrence of these reactions within the cell would be problematic. Indeed, the RidA paradigm highlights the difficulty of inferring cellular function from studies of proteins in isolation. In fact, this study highlights the requirement to better define the differences between the test tube and the cell. The effect of RidA on 2-AA hydrolysis cannot be observed *in vitro* at neutral pH because it breaks down too rapidly [4]. Additionally the *in vitro* inactivation of IlvE needed to be performed at a pH of 9.5 to obtain suitable inactivation [7]. These high pH levels are not present in the cell where the protecting effect of RidA can be seen. This pH requirement raises the question, what about the cellular environment differs so much from the test tube?

Previously we have suggested that there exists a low availability of free water within the cell [4] that lends itself to longer half-lives of enamines *in vivo*. Upon close look, it seems unlikely that this is the sole contributing factor. The inside of the cell has a relatively high concentration of ions (>0.1 M) [12]. The effect of ionic strength on the half-life of 2-AA has not been reported and may be worth inquiry. Also, the landscape of the cell is quite different from the test tube with protein densities that approach 400 mg mL^{-1} [13] and non-uniform distribution of enzymes [12]. These two factors result in a greatly different diffusional properties within the cell. It is possible that increased 2-AA inhibition occurs within the cell because it has less distance to travel through aqueous solution to encounter an enzyme to inhibit.

It is humbling that the identification of a protein with such a profound effect on cellular physiology required so many years of study of cellular physiology to be uncovered. In the genomics age, studies like these become increasingly important. The number of genes of unknown function is ever increasing and defining their activities is essential to identifying

metabolic potential from genome sequences. The study of cellular physiology is still ripe with discoveries to be uncovered about life.

4.4 REFERENCES

1. Browne, B.A., A.I. Ramos, and D.M. Downs, *PurF-independent phosphoribosyl amine formation in yjgF mutants of Salmonella enterica utilizes the tryptophan biosynthetic enzyme complex anthranilate synthase-phosphoribosyltransferase*. J Bacteriol, 2006. **188**(19): p. 6786-92.
2. Enos-Berlage, J.L., M.J. Langendorf, and D.M. Downs, *Complex metabolic phenotypes caused by a mutation in yjgF, encoding a member of the highly conserved YER057c/YjgF family of proteins*. J Bacteriol, 1998. **180**(24): p. 6519-28.
3. Schmitz, G. and D.M. Downs, *Reduced transaminase B (IlvE) activity caused by the lack of yjgF is dependent on the status of threonine deaminase (IlvA) in Salmonella enterica serovar Typhimurium*. J Bacteriol, 2004. **186**(3): p. 803-10.
4. Lambrecht, J.A., J.M. Flynn, and D.M. Downs, *Conserved YjgF protein family deaminates reactive enamine/imine intermediates of pyridoxal 5'-phosphate (PLP)-dependent enzyme reactions*. J Biol Chem, 2012. **287**(5): p. 3454-61.
5. Stauffer, G.V., *Biosynthesis of Serine, Glycine, and One-Carbon Units*, in *Escherichia coli and Salmonella typhimurium Cellular and Molecular Biology*, F.C. Neidhardt, Editor 1996, American Society for Microbiology: Washington. p. 506-513.
6. Wang, E.A., R. Kallen, and C. Walsh, *Mechanism-based inactivation of serine transhydroxymethylases by D-fluoroalanine and related amino acids*. J Biol Chem, 1981. **256**(13): p. 6917-26.

7. Lambrecht, J.A., G.E. Schmitz, and D.M. Downs, *RidA proteins prevent metabolic damage inflicted by PLP-dependent dehydratases in all domains of life*. MBio, 2013. **4**(1): p. e00033-13.
8. Cicchillo, R.M., et al., *Escherichia coli L-serine deaminase requires a [4Fe-4S] cluster in catalysis*. J Biol Chem, 2004. **279**(31): p. 32418-25.
9. Zhang, X. and E. Newman, *Deficiency in l-serine deaminase results in abnormal growth and cell division of Escherichia coli K-12*. Mol Microbiol, 2008. **69**(4): p. 870-81.
10. Tani, T.H., et al., *Adaptation to famine: a family of stationary-phase genes revealed by microarray analysis*. Proc Natl Acad Sci U S A, 2002. **99**(21): p. 13471-6.
11. Newman, E.B. and R. Lin, *Leucine-responsive regulatory protein: a global regulator of gene expression in E. coli*. Annu Rev Microbiol, 1995. **49**: p. 747-75.
12. Spitzer, J., *From water and ions to crowded biomacromolecules: in vivo structuring of a prokaryotic cell*. Microbiol Mol Biol Rev, 2011. **75**(3): p. 491-506, second page of table of contents.
13. Ellis, R.J. and A.P. Minton, *Cell biology: join the crowd*. Nature, 2003. **425**(6953): p. 27-8.

APPENDIX A

Structural explorations into RidA mechanism

The following chapter is a compilation of my theories concerning the activity of RidA at a molecular level. In the manuscript, *Conserved YjgF Protein Family Deaminates Reactive Enamine/Imine Intermediates of Pyridoxal 5'-Phosphate (PLP)-dependent Enzyme Reactions*, I was heavily involved with the development of the model for enzymatic activity. The details that follow represent the evolution of my ideas as they differ from the manuscript above. Much thanks goes to Dr. Jennifer Lambrecht for constructing the site directed mutants and evaluating enzyme activity referenced here.

A.1. Introduction

The RidA substrates 2-aminoacrylate and 2-aminocrotonate are generated within the cell by PLP-dehydratases [1, 2] and amino acid oxidases [3]. The instability of these molecules in aqueous solutions, where they are readily hydrolyzed and deaminated by water has been discussed previously throughout this body of work.

In an attempt to elucidate a function for the highly conserved RidA family of proteins, numerous structural studies have been undertaken [4-6]. These studies revealed a homotrimeric structure containing a cavity located at the subunit interfaces that was decorated with seven totally conserved residues. Nuclear magnetic resonance spectroscopy further revealed that a RidA homolog was able to bind 2-ketobutyrate (2KB) and analogs of its enamine: tiglate, methacrylate and ketoisovalerate [4]. Though a biochemical activity was not obtained, the substrates that bound RidA suggested it to be an enamine deaminase [4].

Following the finding that RidA was an aminoacrylate/aminocrotonate deaminase by Dr. Jennifer Lambrecht [7], we re-evaluated the RidA active site informed by an activity to elucidate the mechanism by which the RidA active site facilitates efficient hydrolysis of enamines. The following chapter details my current hypotheses concerning the mechanisms of RidA activity at a molecular level. The proposed mechanism of RidA activity presented here differ from the published manuscript as my theories have evolved. The activity data discussed here can be seen in its entirety in the published manuscript *Conserved YjgF protein family deaminates reactive enamine/imine intermediates of pyridoxal 5'-phosphate (PLP)-dependent enzyme reactions* [7]. Dr. Lambrecht performed the site-directed mutagenesis and evaluation of the mutant activities.

A.2. TdcF Crystal structure

After the discovery of enamine deaminase activity of RidA, the crystal structures obtained for TdcF from *E. coli*, (73% identity to RidA) obtained by Burman *et. al* were investigated to attempt to obtain insight on the molecular mechanism for activity [6]. The model of TdcF is the best published structural data for any member of the RidA family and has all of the highly conserved residues. Consequently it serves as a good representative of the family. The crystal structures were obtained in the absence of ligand and in the presence of 2-ketobutyrate. The putative active-site bound ketobutyrate (Figure A.1) with the arginine 105 coordinating the carboxylic acid. Additionally, the hydrogen bonding scheme with cysteine 10 and glutamate 12 suggested that the molecule is bound in the enol form instead of being bound in solution stable the carbonyl form. The active site pocket also had an ordered water bound adjacent to the alpha carbon with a number of hydrogen binding partners.

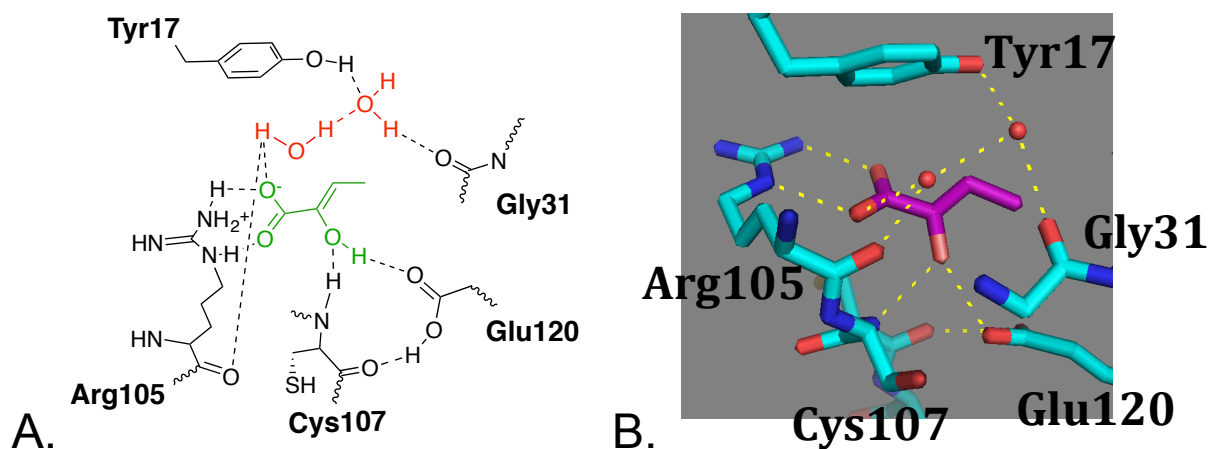


Figure A.1. The active site configuration of TdcF. A, The molecular diagram showing the putative hydrogen bonding network of 2-ketobutyrate (green) bound in the enol form with waters (red) within the active site of TdcF. B, the crystal structure model (PDB 2UYN) shows the

spatial orientation of the of 2-ketobutyrate (fuschia) bound in the active site with water molecules (red spheres) and putative active site residues (cyan sticks). Inferred hydrogen bonding is shown with dotted yellow lines.

A.3. RidA activity in light of crystal structure

When considering the active site with 2KB bound, the enamine intermediate, 2-aminocrotonate, may bind in a similar orientation as the 2KB. This would make the nitrogen available for hydrogen binding at cys107/glu120. I suggest that the H-bond to glu120 and the H-bond to cys107 stabilizes the formation of a hybrid intermediate that is in between an imine and enamine (Figure A.2 [I]). The placement of the water molecule is directly adjacent to the alpha carbon, lying 2.7 Å perpendicular to the ligand in the 2KB crystal structure. Additionally, the hydrogen bonding scheme of the water could serve to make it a stronger nucleophile thorough H-bonds with Arg105, the carboxylic acid of the substrate and an adjacent water molecule. This arrangement may allow for hydrolysis while circumventing a tautamerization; water is held at a suitable distance for attack and the beta-carbon lies 2.9 Å from the water molecule where it could obtain a proton in a concerted reaction (Figure A.2 [II]). It is also interesting to note that there is free rotation about the single bond between the alpha carbon and the carboxylic acid, and the carboxylic acid is turned so that it is at an ideal distance to for hydrogen bonding with the water molecule. This placement of the carboxylic acid would also serve to stabilize the hydrolysis transition state (Figure A.2 [III]) by allowing for the formation of a five membered intermediate.

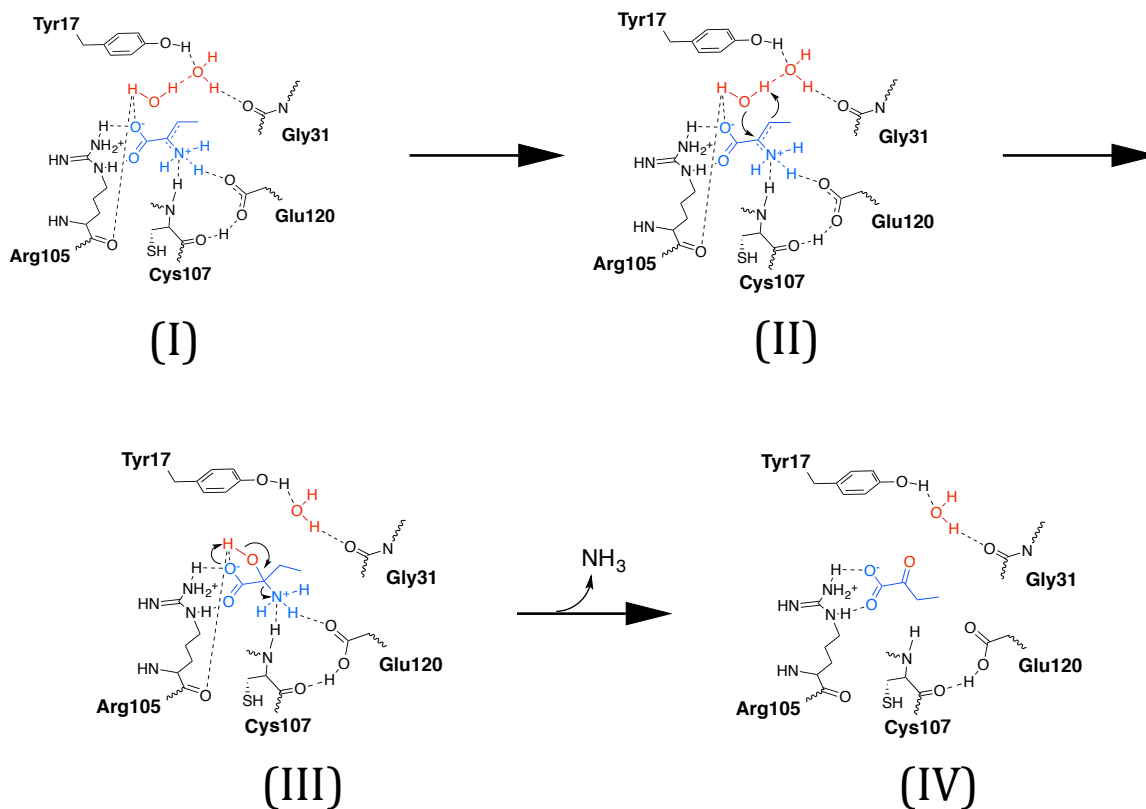


Figure A.2. Proposed mechanism of RidA catalysis of 2-aminocrotonate to 2-ketobutyrate.

The hydrogen bonding of Cys107 and Glu120 may allow for the stabilization of a hybrid enamine/imine intermediate (I) with water ordered at a suitable distance and location for attack at the alpha carbon (II). The tetrahedral intermediate (III) quickly breaks down to the final product, 2-ketobutyrate (IV).

Mutagenesis of three of the highly conserved residues were performed to probe the catalytic mechanism of RidA. The results are given below in Figure A.3. As expected, the mutagenesis of arg105 nearly abolished activity due to the lost hydrogen bonding with the carboxylic acid. The interesting residues are the invariant glu120 and highly conserved tyr17. Mutation of tyrosine to phenylalanine resulted in an approximately 50% decrease in activity at both pH 8.0 and 9.5. The reason for this drop in activity can be explained by the loss of

hydrogen bonding in the model presented above. Tyrosine is positioned to hydrogen bond with the distant water which is H-bonded to the water facilitating the attack. Tyrosine could help position the waters and also make the attacking water more nucleophilic. The mutation of the invariant glutamate was the most interesting; mutation of the glutamate to a lysine showed similar activity as an alanine. This suggests that the acidic character of the glutamate is important to catalysis. This is consistent with our model where the H-bonding of glutamate allows for more electron density available to the beta-carbon, making it more basic. When RidA lacks the acidic glutamate, it could still hold the substrate in the active site adjacent to the water molecule. This could account for the activity seen at pH 8.0. However at higher pH's, the correct positioning isn't enough; activation of the substrate is required as the stability of the enamine increases with pH.

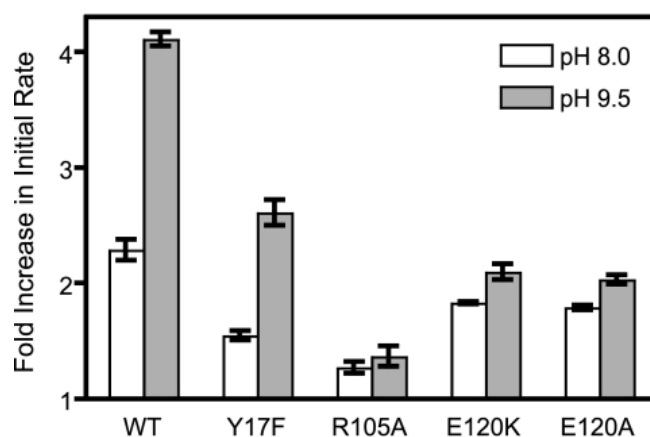


Figure A.3. Activity of RidA variants. The standard assay was described previously [2].

Activity is represented as the fold increase of initial rate vs. threonine dehydratase alone in the absence of RidA. Figure from *Lambrecht, Flynn and Downs*.

A1.4. Future directions

Previously we hypothesized that the activity of RidA was to sequester and activate water to facilitate the attack on the imine. This mechanism would rely on the tautomerization to occur in bulk solvent. More careful evaluation suggests that RidA activity would need to facilitate or circumvent tautomerization to be consistent with the activity observed. If the tautomerization proceeds in bulk solution the hydrogen at the beta-carbon would be added with random stereochemistry. However if the reaction proceeded as it is described above, steric hinderance in the active site would favor the addition on one side of the molecule. In order to probe this, the assay could be performed in deuterated water in a polarimeter. The addition of a deuteron generates a chiral center at the beta carbon. Subsequently we would expect that in the absence of RidA, the enamine would tautomerize with protonations at either face of the beta carbon, producing a racemic mixture that would not rotate polarized light. However, if the addition of RidA resulted in the rotation of polarized light, we can conclude that the addition of the deuteron to the beta-carbon is occurring in an enzyme-facilitated manner.

The synthesis of an analog of the intermediate seen above in Figure A.2 (III) would be helpful for studying binding affinities. Synthesizing an analog with carbon in the alpha position may prove to be difficult so I propose synthesis of a phosphonate molecule with phosphorus in the alpha position as seen in Figure A.4.A. The required substituents on phosphorus of the proposed analog are akin to the structure of the herbicide, glufosinate. Glufosinate is also known as phosphinothricin, a natural product produced by *Streptomyces viridichromogenes* [8].



Figure A.4. The proposed structural analog of the reaction intermediate. The analog (A) has similar substituents on the phosphorus as glufosinate (B).

After the synthesis of the analog and/or others, they can be evaluated for binding to RidA with isothermal calorimetry. When compared to the other known ligands that bind [4], we would expect this intermediate analog to have the greatest binding affinity. Additionally, these molecules could be tested for inhibition of RidA. The expected result would be that they would competitively inhibit RidA activity.

A1.5. References

1. Datta, P. and R. Bhadra, *Biodegradative threonine dehydratase. Reduction of ferricyanide by an intermediate of the enzyme-catalyzed reaction.* Eur J Biochem, 1978. **91**(2): p. 527-32.
2. Lambrecht, J.A., G.E. Schmitz, and D.M. Downs, *RidA proteins prevent metabolic damage inflicted by PLP-dependent dehydratases in all domains of life.* MBio, 2013. **4**(1): p. e00033-13.

3. Walsh, C., et al., *Studies on the mechanism of action of the flavoenzyme lactate oxidase. Oxidation and elimination with beta-chlorolactate.* J Biol Chem, 1973. **248**(20): p. 7049-54.
4. Parsons, L., et al., *Solution structure and functional ligand screening of HI0719, a highly conserved protein from bacteria to humans in the YjgF/YER057c/UK114 family.* Biochemistry, 2003. **42**(1): p. 80-9.
5. Volz, K., *A test case for structure-based functional assignment: the 1.2 Å crystal structure of the yjgF gene product from Escherichia coli.* Protein Sci, 1999. **8**(11): p. 2428-37.
6. Burman, J.D., et al., *The crystal structure of Escherichia coli TdcF, a member of the highly conserved YjgF/YER057c/UK114 family.* BMC Struct Biol, 2007. **7**: p. 30.
7. Lambrecht, J.A., J.M. Flynn, and D.M. Downs, *Conserved YjgF protein family deaminates reactive enamine/imine intermediates of pyridoxal 5'-phosphate (PLP)-dependent enzyme reactions.* J Biol Chem, 2012. **287**(5): p. 3454-61.
8. Hoerlein, G., *Glufosinate (phosphinothricin), a natural amino acid with unexpected herbicidal properties.* Rev Environ Contam Toxicol, 1994. **138**: p. 73-145.

APPENDIX B

The construction of a strain that accumulates 2-aminoacrylate gives evidence for phosphohydroxythreonine transaminase inhibition

B.1. INTRODUCTION

Evidence in Chapter 2 demonstrated that 2-AA is an endogenous metabolic stressor. The main source characterized in *S. enterica* is from the biosynthetic threonine dehydratase, IlvA, which is required for the synthesis of isoleucine in media lacking this essential amino acid. Work here and elsewhere [1] used *ridA* mutants to bolster 2-AA levels in the cell. This has allowed for the identification of four cellular enzymes inhibited by 2-AA *in vivo*. To further understand the effect that 2-AA has in the cell, it would be beneficial to identify and characterize the sum of the enzymes inhibited via 2-AA. The following short chapter details the construction of diagnostic strain intended to overproduce 2-AA through the inducible expression of the degradative threonine dehydratase, TdcB.

The cell has tremendous plasticity and is quite adept at dealing with challenges posed by 2-AA toxicity. This is seen poignantly in the case of GlyA inhibition discussed in Chapter 3. Serine hydroxymethyltransferase activity, the only source of glycine and one-carbon units [2], is inhibited to 20% activity and the only discernable defect is a slight growth defect and pyruvate excretion. For enzymes that are less susceptible to defects, identification of phenotypes may be impossible though they alter cellular physiology. For these enzymes it would be advantageous to have a tool to bolster 2-AA levels in the cell and subsequently exacerbate inhibition to aid in detection of phenotypes.

To this end, I took advantage of activity of the degradative threonine deaminase, TdcB. TdcB is a homolog of IlvA but lacks the domain responsible for allosteric regulation by isoleucine [3]. Consequently when TdcB is present, it is fully active and will continuously dehydrate serine and generate 2-AA. TdcB is contained in an operon containing serine and threonine catabolism genes that is expressed when cells are exposed to serine and threonine.

Interestingly, the Tdc operon in *E. coli* K12 contains a RidA homolog TdcF [4]. The inclusion of a RidA homolog in the Tdc operon is not ubiquitous (not seen in *S. enterica* LT2) but we can postulate that it provides the cell with extra protection from 2-AA when serine is being dehydrated without the feedback inhibition mechanism of IlvA.

This Chapter describes the construction of a strain with a chromosomal insertion of *tdcB* with inducible expression. Using the biosynthetic alanine racemase, Alr, as a probe, this strain shows increased accumulation of 2-AA. Additionally the results give evidence for inhibition of another enzyme, phosphohydroxythreonine transaminase (SerC).

B.2. MATERIALS AND METHODS

B.2.1. Bacterial strains, media, and chemicals.

All strains used in this study are derivatives of *S. enterica* serovar Typhimurium LT2 and are listed with their genotypes in Table B.2 Minimal medium was no-carbon E (NCE) supplemented with 1mM MgSO₄ [5] and 11 mM D-glucose. Difco nutrient broth (NB; 8 g/L) with NaCl (5g/L) was used as a rich medium. Difco BiTek agar was added (15g/L) for solid medium. When required for plasmid maintenance or strain selection, ampicillin was added to minimal and nutrient media at 15 and 150 mg/L, respectively and chloramphenicol was added to rich medium at 15 mg/L. Unless noted, all chemicals were purchased from Sigma-Aldrich Co. (St. Louis, MO).

B.2.2. Molecular Biology

The construction of pBAD *tdcB cat* was constructed in the following steps: (1) *tdcB* was cloned from *S. enterica* genomic DNA into pBAD24 previously by Jennifer Lambrecht to

generate pJL1. (2) the gene encoding chloramphenicol acetyltransferase was cloned from pSU18 using primers JF66 (tagaagcttgagttatcgagatttcagg) and JF67(tagaaacTTAcgccccgccctgccactcatc), cut with *Hind*III and ligated into pJL1 cut with *Hind*III. Resulting colonies were selected for chloramphenicol resistance on media containing arabinose. The resulting plasmid was pBAD *tdcB cat*.

To generate the chromosomal insertion/deletion primers JF68 (cctgaaaaacagcaagaaagcgggtgtaattattgtttatttgcacggcgctcacactt) and JF 69 (tacgttatcccatagcctgctcactctgcccgtcgggtccgcaaaacagccaagct) were used to amplify the *araP* sequence, *tdcB* and *cat* genes. The primers add 40 base pair sequences that correspond to the sequence up and downstream of the *tdc* operon. This DNA fragment was then used in the insertion/deletion technique described previously [6]. The insertion sites were sequenced to verify the correct insertion.

B.2.3. HPLC Quantification of Cofactors

Quantification was performed as previously described in Chapter 2.

B.3. RESULTS

B.3.1. Construction of strain containing with inducible expression of *tdcB*.

To exacerbate the accumulation of 2-AA, a strain was constructed that contained a chromosomal insertion of *tdcB* under expression of the inducible arabinose promoter. The gene encoding the chloramphenicol acetyl-transferase, *cat*, was cloned into pJL1 to generate pJF5 (Figure B.1). This plasmid conferred chloramphenicol resistance when arabinose (0.2% final conc.) was added to the culture medium.

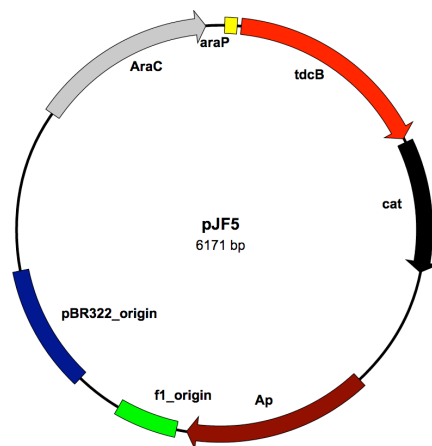


Figure B.1. pJF5 map.

pJF5 is a pBAD24 derivative that contains has arabinose inducible expression of the genes encoding degradative threonine dehydratase (*tdcB*) and chloramphenicol acetyltransferase (*cat*). Plasmid map was generated using Savvy Scalable Vector Map Utility (<http://bioinformatics.org/savvy/>).

Using the insertion/deletion method of Datsenko and Wanner [6], a portion of the plasmid was inserted in place of *tdc* operon. The insert included the arabinose promoter, the genes encoding TdcB and chloramphenicol acetyltransferase. Due to homology of *tdcB* between the insertion, it was possible for recombination events that would not include the entirety of the intended sequence. The construction of this insertion allowed for the verification of the whole insertion by selecting for chloramphenicol resistant colonies in the presence of arabinose and then screening for chloramphenicol sensitivity in the absence of arabinose. This would ensure both the arabinose promoter and the *cat* gene were involved in the recombination. By these criteria, a handful of colonies were isolated and their construction was verified by sequencing the regions of the chromosome where the splicing occurred. One correct strain was saved as DM13621 with the genotype *tdc::araPtdcBcat*. Using p22 transduction, the genetic construct

was transferred to different backgrounds using the selection described above to generate the strains listed in Table B.1.

B.3.2. Strains expressing *tdcB* result in greater 2-AA accumulation in *ridA* mutant strains

Strains containing the *tdcB* insertion described above were generated in the wild type background and *ridA* mutant background in order to ascertain the effect that *tdcB* overexpression had on a *ridA* mutant. To probe the relative accumulation in the tested strains, I used Alr for a probe. In Chapter 2 it was shown that Alr is exposed to 2-AA in *ridA* strains. By comparing the cofactor content of Alr isolated out of *ridA* mutants and *ridA tdc::araPtdcBcat* strains, we can determine if any increased accumulation of 2-AA is occurring.

These strains were transformed with the pJF2 plasmid described in Chapter 2, in order to isolate Alr from these strains. After growth in minimal media, Alr was purified and the cofactor content was analyzed via HPLC. I hypothesized that the expression of TdcB in *ridA* mutant strain would cause more accumulation of 2-AA, increasing the pyruvate/PLP content in the Alr isolated from this strain when compared to a *ridA* mutant alone. The cofactor content is shown in Table B.1. As expected, strains with intact *ridA* showed no sign of 2-AA accumulation. Strikingly, Alr isolated from the *ridA* strain expressing TdcB had less than half the level of pyruvate/PLP compared to *ridA* alone. However, the effect of TdcB is revealed when PLP content is also considered. The total cofactor (PLP plus pyruvate/PLP) content showed a significant difference between the strains: the *ridA* mutant alone has 18.4 nmol/mg while *ridA* mutant in combination with overexpression of TdcB has only 12.4 nmol/mg. This is a drop in 33% of total cofactor, shadowing an observation of *ridA* alone having 5-10% less cofactor compared to wild type.

Isolation Strain	Relevant Genotype	Supplement	PLP (nmol mg ⁻¹)	Pyruvate/PLP (nmol mg ⁻¹)	Total Cofactor (nmol mg ⁻¹)
DM13674	Wild type	-	19.6 ± 2.1	ND	19.6
DM13762	<i>tdc::tdcB</i>	-	18.8 ± 0.6	ND	18.8
DM13675	<i>ridA::MudJ</i>	-	15.7 ± 0.7	2.7 ± 0.2	18.4
DM13740	<i>ridA::MudJ tdc::tdcB</i>	-	11.2 ± 0.9	1.2 ± 0.2	12.4
DM13740	<i>ridA::MudJ tdc::tdcB</i>	pyridoxal	12.0 ± 0.4	3.8 ± 0.2	15.8

Table B.1. Cofactor content of Alr isolated from various strains. Alanine racemase was overexpressed in various strains using pJF2, purified, denatured and analyzed via HPLC.

The lowered amount of cofactor was surprising, as it suggests that 2-AA may have an effect on PLP cofactor biosynthesis. To test this, Alr was isolated from *ridA* strains (plus/minus *tdcB* expression) in the presence of exogenous pyridoxal and the cofactors were quantified as above. In fact, the addition of pyridoxal increased the overall cofactor content and caused the increase in pyruvate/PLP isolated (Table B.1). These results demonstrate that the strain accumulates excess 2-AA and suggest that the excess 2-AA affects pyridoxal biosynthesis.

B.4. CONCLUSIONS AND FUTURE DIRECTIONS

The construction of a strain that accumulates excess 2-AA was successful. The insertion of *tdcB* into the chromosome under control of the arabinose promoter caused an increase in 2-AA as measured by the cofactor content of Alr isolated from relevant strains. This tool was developed to help identify phenotypes related to 2-AA-toxicity. The presentation of these phenotypes can be subtle, subsequently any exacerbation of inhibition will result in more readily

identifiable phenotypes. Serendipitously, while obtaining the proof of principle for this construct, one such phenotype may have been uncovered: the limitation of pyridoxal. Hints of pyridoxal starvation had been shown previously but the increased levels of 2-AA in the constructed strain gave definitive proof. *tdcB* overexpression can now be used in screens to identify more phenotypes -or- once a phenotype has been putatively identified, a quick test to see if they are exacerbated when combined with the *tdc::araPtdcBcat* construct will show if the phenotype is tied to 2-AA.

The defect in pyridoxal biosynthesis will be an interesting *ridA*-dependent effect to track down. There is paradoxically one PLP-dependent enzyme in pyridoxal biosynthesis, phosphohydroxythreonine transaminase (SerC), that catalyzes the final step in serine biosynthesis as well. Because it is the only PLP-dependent enzyme in the biosynthesis of pyridoxal, SerC is a strong candidate for inhibition given the theme of PLP-enzyme inhibition in *ridA* strains. This would give evidence for another bottleneck in one carbon unit and glycine generation, in addition to GlyA inhibition. However, the work performed in Chapter 3 revealed that defects may not be straightforward and may lie in distant branches of the metabolic network. Only thorough characterization of the pyridoxal biosynthetic network will reveal the source of the defect; the tool developed here will help in this effort.

B.5. REFERENCES

1. Lambrecht, J.A., G.E. Schmitz, and D.M. Downs, *RidA proteins prevent metabolic damage inflicted by PLP-dependent dehydratases in all domains of life*. MBio, 2013. 4(1): p. e00033-13.

2. Matthews, R.G., *One-carbon metabolism*, in *Escherichia coli and Salmonella typhimurium Cellular and Molecular Biology*, F.C. Neidhardt, Editor 1996, American Society for Microbiology: Washington. p. 506-513.
3. Simanshu, D.K., et al., *Crystallization and preliminary X-ray crystallographic analysis of biodegradative threonine deaminase (TdcB) from Salmonella typhimurium*. Acta Crystallogr Sect F Struct Biol Cryst Commun, 2006. 62(Pt 3): p. 275-8.
4. Burman, J.D., et al., *The crystal structure of Escherichia coli TdcF, a member of the highly conserved YjgF/YER057c/UK114 family*. BMC Struct Biol, 2007. 7: p. 30.
5. Davis, R.W., D. Botstein, and J. R. Roth, *Advanced bacterial genetics*. 1980, Cold Spring Harbor, N.Y.: Cold Spring Harbor Laboratory.
6. Datsenko, K.A. and B.L. Wanner, *One-step inactivation of chromosomal genes in Escherichia coli K-12 using PCR products*. Proc Natl Acad Sci U S A, 2000. 97(12): p. 6640-5.